CHAPTER THREE

LITHOLOGY

Chapter Three

Lithology

Lithologic description, analysis of sedimentary structures manifested with both field and core photographs, and granulometric analysis of the studied surface and subsurface rocks are the main topics treated in this chapter. The vertical variation and modification in the sedimentary structures within the studied sections are useful tools for recognizing the mode of sediment transport and the related depositional environments.

3.1 Rock units

3.1.1 Surface section

A sedimentary section at Gebel Naqus to the north of El Tor was measured and sampled. The section is about 370 m thick and is represented by the entire Naqus Formation (Upper Cambrian) and the uppermost part of the underlying Araba Formation (Lower Cambrian). Figure 3.1 shows a panoramic view of the sequence, and the lithologic description of the sedimentary succession is shown in Figure 3.2. A description of each formation is given below.

3.1.1.1 Araba Formation

Araba Formation (Early Cambrian) unconformably overlies pink granites cut by numerous dykes. The formation (15 m thick) consists mainly of very fine- to fine-grained, moderately- to moderately-well sorted, semi-friable to well-cemented sandstone which is found in a series of varicolored beds (PL. 3.1A, B). These varicolored sandstones are composed of 10-80 cm bodies of different colors. Ferruginous materials and yellowish streaks of clay matter are frequently observed along the

Fig. 3.1: Panoramic view of the measured sedimentary succession at Gebel Naqus showing Araba and Naqus formations. The maximum thickness of the exposed rocks is approximately 370 m.

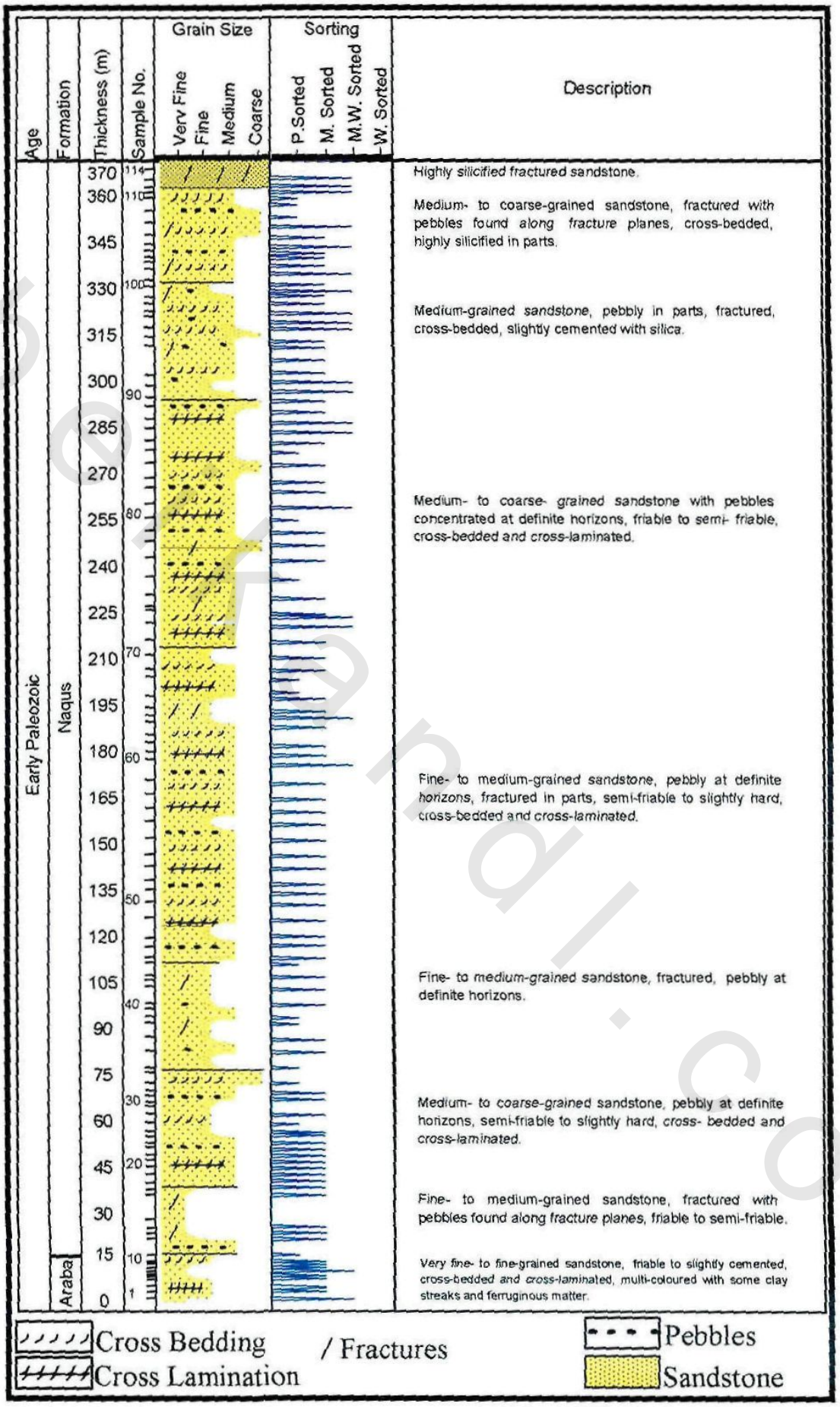

Figure3.2: Lithological description of the Gebel Naqus sedimentary succession (according to the present study).

lamina planes throughout the formation (PL. 3.1C, D). Chemical structures are represented by color banding (liesegang bands) and mottling (PLs. 3.1C, D; 3.2A). The common biogenic structures characterizing the formation are *Skolithos* tubes penetrating the beds for several centimeters (PL. 3.2B).

3.1.1.2 Naqus Formation

Naqus Formation (Late Cambrian) conformably overlies Araba Formation. The formation (355 m thick) consists of a sequence of white to pale brownish, massive, laminated and cross-bedded, jointed and fractured, fine- to medium grained (occasionally coarse-grained), moderately- to moderately-well sorted (occasionally poorly sorted), subangular to subrounded, friable to highly-cemented sandstone. Numerous quartz pebbles and cobbles are both randomly distributed in Naqus Sandstone and preferentially oriented along the foreset lamina and/or the bases of its cross-bedding (PL. 3.2C, D). The topmost part of the formation (1-4 m) is highly jointed and is strongly cemented by silica. This part has the characteristics of pedogenic silcretes (PL. 3.3A, B).

Naqus Formation exhibits less color variations than the underlying multi-colored sandstone of Araba Formation. There are other significant differences between the two formations. Naqus Formation is cross-bedded, highly jointed, dissected, poorly cemented and has high porosity and permeability, whereas Araba Formation is multi-colored, highly cemented and has low porosity and permeability. This drastic difference is an aid for identifying the contact between the two formations.

An east-west oriented igneous dyke is recorded in the studied area (PL. 3.3C). The age of this igneous intrusion is pre-Carboniferous as it cuts through the Early Paleozoic Araba and Naqus formations along deep-seated fault plane and does not affect the sedimentary rocks of younger

age. The stratigraphic succession of these units in the studied area is highly dipping away from the dyke. The Cambrian sediments were halted by magma intrusion, which terminate the early stage of this type of sediments in the area (oldest formation of rocks in Sinai). This invasion probably marks an episode of tectonic magmatic intrusion that prevailed over the area for a long time, culminated in the most widespread Erythrean faults (cf. Issawi et al., 1981).

3.1.2 Subsurface section

The Nubia Sandstone Unit I reservoir is located approximately 12,000 ft below sea-level and forms a part of a sequence of Paleozoic sediments unconformably rest on a Precambrian peneplain. The reservoir comprises predominantly massive, mature quartz sandstones and occasional minor shales and polymictic conglomerate horizons, probably indicates a significant unconformity, with red claystone and white sandstone clasts and granules (PLs. 3.3D, E; 3.4A). Some of the recorded clasts have been deformed prior to lithification in the present rock. The presence of red claystone clasts in the polymictic conglomerates at different horizons indicates that there are at least two red claystone units of different ages, in the area, although they cannot be accurately dated. Some of the sandstone clasts in the conglomerates have a hematitic cement.

The sandstone is light tan, brownish gray to green, fine to coarse and occasionally very coarse grained, poorly to well sorted, subangular to rounded and well cemented by kaolinitic and siliceous cements. Occasionally, ferruginous, calcareous and halite cements are also observed. Some horizons are oil stained and/or have residual bitumen in the original pores (PL. 3.4B, C). More than 98 % of the grains are quartz with a very rare feldspar, tourmaline and zircon minerals recorded. Rutile

and white mica are also seen occasionally. In hand specimens, extensive quartz veining is apparent (PL. 3.4B).

Fractures without noticeable displacement are very common in the cores of Unit I (PL. 3.4). Thin sections show that these fractures are filled with crushed quartz grains. If shale is present in the surrounding rock, this also forms part of the fracture fill. Relatively infrequent open (conductive) fractures are also recorded (PL. 3.4C). A characteristic feature of wells producing from the Paleozoic Sandstone is the low productivity index and the high positive skin factor. This is presently attributed to abundant quartz veins, which are believed to act as permeability barriers (Harper, 1984).

3.2 Sedimentary structures

According to Pettijohn and Potter (1964) "the structure is an inherent property of a rock and a guide to its origin". A sedimentary structure refers to internal megascopic morphological features. These features have been studied for some time, as they are often visible to the naked eye. They include the thickness and the shape of beds, their internal organization, the nature of their surfaces, joints, concretions, cleavages, and fossil content.

Sedimentary structures are arbitrarily divided into primary and secondary classes. Primary structures are those generated in a sediment during or shortly after deposition and subject to no applied forces other than gravity. Secondary sedimentary structures are those, which formed sometime after sedimentation as a result of externally applied forces in addition to gravity. They result essentially from chemical processes, such as those, which lead to the diagenetic formation of concretions.

Classification of sedimentary structures can be based on the time of their formation (Selley, 1988). They are defined as: (a) predepositional

structures, occur on surfaces between beds, and are formed before the deposition of the overlying bed. This group of structures consists largely of erosional features such as scour and fill, flutes and grooves. These structures are sometimes collectively called sole marks or bottom structures, (b) syndepositional structures, formed actually during sedimentation. They are, therefore, essentially constructional structures which are present within sedimentary beds. These structures contain information on, physical, chemical or biological conditions, existing in a depositional environment during sedimentation. They are subdivided into inorganic and organic structures, depending on their origin, and (c) postdepositional structures, formed due to deformation and are oftenly of chemical origin. Their occurrence reflects diagenetic phenomena or physical origin resulting from tectonic deformation. A second classification may be based on the agents or processes that have created the sedimentary structures, in this concern, this classification includes: physical, chemical and biochemical types. A third classification of sedimentary structures based on their location can be suggested, and includes external structures and internal structures.

In the present work, the purpose of this section is to recognize the sedimentary structures of the investigated sandstones as a trial to establish their significance for environmental interpretation. The following structures are recognized:

3.2.1 Primary sedimentary structures

3.2.1.1 Biogenic structures

Biogenic structures are generated by organic processes (organisms). They include plant rootlets, vertebrate footprints (tracks), trails (due to invertebrates), soft sediment burrows and hard rock borings. These phenomena are collectively known as trace fossils and their study is

referred to as ichnology. The shape of a trace fossil reflects environment rather than creator. This means that trace fossils can be very important indicators of the origin of the sediment in which they are found because of their close environmental control. Furthermore, trace fossils always occur in situ and cannot be reworked like most other fossils (Selley, 1988).

An individual morphological type of trace fossil is termed an ichnogenus. The various types of ichnogenera cannot be grouped phyllogenetically because various organisms produce similar traces. Ichnofossils have been grouped according to the activity which made them (Seilacher, 1964) or according to their topology (Martinsson, 1965). The topological scheme essentially describes the relationship of the trace to the adjacent beds.

The most useful aspect of trace fossils is the broad correlation between depositional environment and characteristic trace fossil assemblages, termed ichnofacies. Schemes relating ichnofacies to environments have been drawn up by Seilacher (1964, 1967), Rodriguez and Gutschick (1970) and Heckel (1972).

In the present study, biogenic sedimentary structures are observed in both Araba and subsurface sandstones (PLs. 3.2B; 3.5A-C), where they are represented by Skolithos tubes (PL. 3.2B). They are deep vertical, tube-like, epichnial endichnial burrows with structureless fill that are believed to have been formed by tube-dwelling organisms that lived in rapidly moving water and shifting sands. Most of the tubes are 1-5 mm in diameter and have several centimeters length. Locally iron crusts coat the *Skolithos* tubes. Occasionally, intense burrowing (termed bioturbation) leads to the progressive disruption of bedding until uniformly mottled

sand is left. This is a characteristic feature of intertidal and subtidal sand bodies (cf. Selley, 1988).

The characteristics of these burrows suggest a rapidly shifting substrate that requires organisms to dig deep vertical burrows that must be rebuilt often when waves wash them away. Most of the burrowing organisms appear to be filter feeders that use the sediment strictly for shelter, not as a source of food. In addition, sedimentological evidence also places this ichnofacies in shallow marine environments. Thus, the *Skolithos* ichnofacies clearly indicates clean, well-sorted near-shore sands with high levels of wave and current energy (intertidal zone).

The organism that made *Skolithos* is unknown, although some geologists have suggested phoronids (a burrowing wormlike lophophorate related to brachiopods) or tube worms. It is also possible that the trace-maker is extinct, since *Skolithos* is unknown after the Cretaceous.

3.2.1.2 Inorganic structures

3.2.1.2.1 Predepositional structures

3.2.1.2.1.1 Erosional surfaces

The contact between the studied sandstones and the underlying basement rocks is a sharp erosional surface. The sediments above the contact are severely cut and eroded into discontinuous strata. Such finding suggests high energy storm events (cf. Brenchley et al., 1979; Harms, 1975).

3.2.1.2.1.2 Channel-fill structures

Channels of different sizes and shapes are recorded in Naqus and Araba formations. The channels are filled with fine-grained, planar and cross bedded sediments. In Araba Formation, theses sediments were later subjected to coloration (PLs. 3.1A; 3.5D; 3.6A, B).

3.2.1.2.2 Syndepositional structures

3.2.1.2.2.1 Massive bedding

Massive beds have no apparent internal structure. It is first necessary to ascertain that this really is the case, and that it is not simply due to surface weathering. It is much more difficult to establish the absence of a feature (in this case lamination) than its presence. Massive bedding is recorded at different parts of Naqus Formation (PL. 3.6C) and different intervals in the subsurface sandstone (PLs. 3.3D; 3.4C). Structureless units, especially thick sandstone beds, may reflect depositional conditions (formed by whether certain sedimentary processes, such as gravity flow, which lack a mechanism to produce primary structures) or it may be due to the destruction of original lamination (Collinson and Thompson, 1982). Lamination may be destroyed by such processes as bioturbation, recrystalization, dewatering (upward movement of pore water), or even by a massive sudden sedimentation which has completely destroyed all traces of stratification.

3.2.1.2.2.2 Graded bedding

A graded bed is one in which there is a vertical gradation change in grain size. Two types of grading are considered, those are normal and reverse grading. Normal grading is marked by an upward decrease in grain size, while reverse (or inverse) grading is where the bed coarsens upward. In the present study, grading is a very ubiquitous feature in Naqus Formation, which can be seen as a sequence of fining upward cycles. Normal grading (PLs. 3.6D; 3.7A) is the most common grading type and is displayed by an upward decrease in grain size (fluvial deposits). The grain size change has two forms: content grading where the mean grain size of the sediment decreased upwards; and coarse tail grading where the size of the coarsest grains decreased, the rest of the population remained roughly constant. Herein, grading is commonly associated with cross-bedding (PLs. 3.6D; 3.7A). Elongated to rounded

pebbles/cobbles and gravels with either irregular distribution or preferred orientation along the foreset lamina planes are mixed with sand grains of other size grades in the lower part of the graded sets. Normal grading reflects the deceleration of the sediment-laden current and the consequent decline in its competence, with coarse grains settling first (Collinson and Thompson, 1982).

3.2.1.2.2.3 Flat bedding (Planar lamination)

The term "planar lamination" is used to describe strata with little or no primary dip i.e. which parallels the major bedding surface. In the studied sandstones, planar stratification is a ubiquitous feature (PLs. 3.2A; 3.7B-E), particularly at the lowermost part of the surface section (Araba Formation) where it forms a fine-grained horizontal channel-fill deposits (PL. 3.5D). Most probably, these deposits have been formed under high flow velocity and shallow water depth conditions (upper flow-regime).

3.2.1.2.2.4 Cross bedding

Cross bedding is one of the most common and most important of all sedimentary structures. It is ubiquitous in traction current deposits in diverse environments (Selley, 1988). It is a very characteristic feature in the studied sandstones and is mainly recognized as sets of small to medium scale (in both surface and subsurface sections), occasionally of large scale (mainly in Naqus Formation). It has been produced by migration of bedforms mainly ripples, megaripples and sand waves. Cross bedding is described here as tabular (both planar and tangential), flaser, lenticular and wavy cross bedding.

Tabular cross bedding was recognized in small to medium scale, where the planar sets are thin with steeply dipping cross laminae attaining angles up to 30°(PLs. 3.7A, F-H; 3.8A, B). Set boundaries are characterized as being either planar or parallel, although in some cases they are somewhat undulatory and convergent. Occasionally, the foresets of tabular sets are

asymptotic (tangentially based) giving rise to tangential tabular cross bedding (PLs. 3.6A, B; 3.8C).

Flaser, lenticular and wavy bedding are recorded only in the subsurface section (PL. 3.9A-C). In areas of ripple formation, the ripples of silt and sand move periodically and mud is deposited at other times. Flaser bedding is where cross lamination contains mud streaks, usually in ripple troughs. With gradually increasing sand content, flaser bedding can grade into beds composed entirely of cross laminated sand in which ripple profiles are absent, though they are sometimes preserved on the top of the bed (Selley, 1988). Lenticular bedding is where mud dominates and the cross lamination occurs in sand lenses. Wavy bedding is where thin ripple cross laminated beds alternate with mudrock (Tucker, 1982). These bedding types are common in tidal flat and delta front sediments, wherever there are fluctuations in sediment supply or level of current (or wave) activity (Tucker, 1982).

3.2.1.2.2.5 Cross lamination

Cross lamination is a synonym of cross bedding, the only difference is in the size. Cross lamination has a set height of less than 6 cm and the thickness of the cross laminae is only a few millimeters, while cross bedding is characterized by set height generally greater than 6 cm and the individual cross beds are many millimeters to a centimeter or more in thickness (Tucker, 1982). Fine scale cross lamination is a common feature in the studied surface and subsurface sandstones (PLs. 3.8D; 3.9D). In Naqus Formation, the laminae are laterally discontinuous, faint and weak in this white sandstone. Basal contacts are sharp and flat with local channeling, while upper contacts are sharp with local grading. The presence of the pebbly coarse sand may indicate a fall in the stream power. On the other hand, the laminae in Araba Formation are laterally

continuous and can be traced for long distance. They are commonly amalgamated with colored sand bodies, which render the laminae sharp and distinct. These fine laminae reflect slow rate of accumulation and minor fluctuation in the velocity of the depositing currents (cf. Hunter and Clifton, 1982).

3.2.1.2.3 Postdepositional structures

3.2.1.2.3.1 Convolute bedding and recumbent foresets

These are postdepositional sedimentary structures due to physical deformation. They occur commonly in single beds of sand or silt in a wide range of environmental settings (cf. Collinson and Thompson, 1982). Convolute bedding and recumbent foresets are mainly recorded at the middle and uppermost parts of Naqus Formation. They are characterized by complex intricate folding of lamina, commonly into upright cuspate forms with sharp anticlines and more gentle synclines (PL. 3.10A-C). The structures have limited lateral extension. Convolution usually increases in intensity upwards through a bed from undisturbed lamination at the base. At the top it may either die out gradually or be sharply truncated. Often associated with convolute bedding is the deformation of cross-bedded sands. The foresets become overturned down-current in the shape of recumbent folds (PL. 3.10C). Recumbent foresets, like convolute bedding, are found in divers traction deposited sands, and are especially common in the coarse sands of braided alluvium (Selley, 1988). The main use of convolute bedding is as evidence of rapid deposition (Collinson and Thompson, 1982).

Considerable attention has been paid to the origin of convolute bedding and recumbent foresets (e.g. Allen and banks, 1972; Mills, 1983; van Loon and Brodzikowski, 1987). There is a widespread agreement that these structures are caused by the vertical passage of water through loosely packed sand. This water may be due to a hydrostatic head of

water, as for example on an alluvial fan (Williams, 1970). Alternatively, the water may be derived from the sediment itself. A sand will not compact significantly at the surface, but its grains may be caused to fall into a tighter packing. This results in a decrease in porosity. Excess pore water will be vertically expelled (Selley, 1988). Other processes that have been suggested include: 1) shearing by currents on a sediment surface, 2) frictional drag exerted by moving sand 3) loading contemporaneous with deposition and 4) lateral laminar flow of liquefied beds.

3.2.2 Secondary sedimentary structures

3.2.2.1 Chemically induced structures

3.2.2.1.1 Differential coloration

This phenomenon is controlled by the grain size distribution, which affects porosity characteristics. It is observed mainly in Araba Formation (PL. 3.1A, B) and is attributed to the presence of iron and manganese minerals with different degrees of oxidation and reduction. Coloration is most probably due to diagenetic alterations (cf. Nelson, 1982).

3.2.2.1.2 Color banding

Color banding (liesegang bands) and mottling is one of the most common chemical structures in the studied sandstones, especially in Araba Formation (PLs. 3.1C, D; 3.2A). It is due to a rhythmic precipitation of iron oxides in thin, closely spaced layers. It reflects the intensity of the stream carrying different chemically saturated elements, especially iron oxides and silica. Bands of red and brown hematite and goethite alternate with white and yellow bands in thin closely spaced layers, many of which are curved and cut across bedding, typical of liesegang bands. It closely mimics bedding lamination, for which it may be mistaken.

3.2.2.1.3 Calcite and gypsum veinlets

These veinlets are recorded in both Naqus and Araba formations (PLs. 3.3B; 3.6C). They are due to the precipitation of these minerals from the circulating brine, filling cavities, fractures and joint planes in the hosted layers.

3.2.2.1.4 Silica-filled fractures

The Paleozoic Nubian Sandstone in Unit I of Ras Budran reservoir is characterized by the presence of crosscutting quartz-rich planar structures, which have the appearance of quartz veins in hand specimen (PLs. 3.3D, 3.4A, B). Under the microscope, the planar structures are seen to be composed predominantly of poorly sorted cataclastic quartz fragments, many of which are very fine grained. They are not strongly defined in thin section, and sometimes branch to form several subparallel features which are commonly of the order of only a single grain diameter in width. Clay minerals are normally not present. Using SEM, small authigenic quartz crystals are detectable. If shale is present in the surrounding rock, this also forms part of the fracture fill. The planarity and nature of the filling of these structures demonstrate that they are shear fractures filled by fine grained cataclastic debris which has become cemented by quartz overgrowth.

Well RB-A5 Unit I core was examined to assess the frequency and mutual orientation of these filled fractures. They were observed to occur once every 7-10 cm when measured along the core axis. No fracture terminations were observed which suggests considerable persistence. The fractures were found to be generally subparallel but at least 25 % deviated from this subparallelism. The majority of the filled fractures appeared to be subvertical, but a proportion with a variety of other inclinations are also present. Fracture length is unknown, but in the absence of visible terminations of fractures in the Well RB-A5 core, it is assumed that the

fracture length is characteristically greater than 10 core diameters. The spacing observed in the core (7-10 cm) suggests that the filled fractures are spaced at distances less than the length of a perforation tunnel.

The permeability of theses structures is substantially less than 10 % of the permeability of the surrounding reservoir sandstone. Consequently, it was concluded that the filled fractures represent significant barriers to fluid flow and are responsible for the low productivity index and the high positive skin factor characteristic of wells producing from the Paleozoic Sandstone. Few wells, which do not show a high positive skin factor, may reflect either a lack of filled fractures or an increase in the number of open fractures.

Open or conductive fractures (without filling) were also observed in the subsurface sandstone (PL. 3.4F), but filled fractures were almost everywhere at least twice as numerous as the open fractures, and about four times as numerous in Unit I. Moreover, because this stated frequency of filled fractures was determined by visual observation of core it is an underestimation because the fractures are sometimes only detectable in thin section. In Unit I sandstones, inspection of cores from four wells revealed that the frequency of filled fractures was approximately four fractures per foot of core length.

3.2.2.2 Mechanically induced structures

3.2.2.2.1 Differential weathering

This sedimentary feature, observed in both Naqus and Araba formations, is mainly due to erosion of the sediment surfaces by the flowing current (PL. 3.7B). The differential erosion of the sediment surface is achieved either by the abrasive action of the larger shape grains suspended in the eddies or by the direct action of the fluid stream. It indicates high power erosive phase of the current (cf. Reineck and Singh,

1980). Differential weathering may have also resulted from the differential erosion of the wind (PLs. 3.3C; 3.8A; 3.10D).

3.2.2.2.2 Joints

Joints are the most common secondary structures recorded in the surface sandstones, particularly in Naqus Formation (PLs. 3.7C; 3.8B). They have variable magnitudes, strike trends and dip directions. They range in length from few centimeters to several meters. Their width is proportional to their length. Though most of these joints are straight and vertical, yet some joint planes are curved exhibiting sinuous character. Most of the straight and vertical joints are open and are mostly recorded in the middle and uppermost parts of Naqus Formation. On the other hand, most of the crossed and sinuous joints are closed, being filled with fine materials and/or calcite and gypsum cements.

3.3 Granulometric composition

Grain size analysis was carried out for hundred and four samples using the conventional method described in chapter 2. Grain size data are graphically presented as histograms and cumulative frequency curves (Figs. 3.3-3.5). The four statistical parameters namely: the graphic mean (Mz), the inclusive graphic standard deviation (σ_I), the inclusive graphic skewness (Ski) and the graphic kurtosis (Kg) were calculated for each sample from the grain size data according to the equations quoted by Folk and Ward (1957). The seven percentiles from which the parameters were calculated, together with the numerical values of the calculated parameters are cited in Table 3.1. Summary of the grain size parameters is shown in Table 3.2 and Figure 3.3. Bivariate relationships between these parameters are illustrated in Figure 3.6.

Table 3.1: Phi (Φ) values and computed grain size parameters for the studied sandstone samples.

S. No.	Φ1	Φ5	Φ16	Φ25	Φ50	Φ75	Φ84	Φ95	Md	Mz	σ_I	Sk_I	K_G
1- Araba Formation													
1	1.93	2.25	2.50	2.62	2.86	3.47	3.90	4.23	2.86	3.09	0.65	0.43	0.95
2	1.15	1.55	1.93	2.19	2.83	3.81	4.08	4.29	2.83	2.95	0.95	0.11	0.69
3	0.91	1.27	1.65	1.85	2.38	3.08	3.58	4.15	2.38	2.54	0.92	0.24	0.96
4	1.27	1.62	1.92	2.15	2.69	3.65	4.04	4.27	2.69	2.88	0.93	0.23	0.72
5	1.20	1.62	2.04	2.25	2.65	3.12	3.42	4.06	2.65	2.70	0.71	0.14	1.15
6	1.48	2.04	2.47	2.69	3.19	3.88	4.05	4.29	3.19	3.24	0.74	0.03	0.77
7	1.81	2.15	2.47	2.62	2.97	3.54	3.81	4.15	2.97	3.08	0.64	0.22	0.89
8	1.53	1.85	2.23	2.54	3.17	3.81	4.04	4.27	3.17	3.15	0.82	-0.06	0.78
9	0.69	1.38	2.12	2.73	3.59	4.10	4.17	4.38	3.59	3.29	0.97	-0.45	0.90
10	1.15	1.58	1.98	2.23	2.71	3.92	4.10	4.31	2.71	2.93	0.94	0.24	0.66
11	0.65	1.13	1.56	1.77	2.38	3.31	3.83	4.19	2.38	2.59	1.03	0.23	0.81
Max	1.93	2.25	2.50	2.73	3.59	4.10	4.17	4.38	3.59	3.29	1.03	0.43	1.15
Min	0.65	1.13	1.56	1.77	2.38	3.08	3.42	4.06	2.38	2.54	0.64	-0.45	0.66
Avg	1.25	1.68	2.08	2.33	2.86	3.61	3.91	4.24	2.86	2.95	0.85	0.12	0.84
2- Naqus Formation													
12	0.36	0.86	1.23	1.41	1.77	2.23	2.55	3.41	1.77	1.85	0.72	0.23	1.27
13	0.07	1.02	1.44	1.64	2.09	2.59	2.82	4.05	2.09	2.12	0.80	0.18	1.31
14	0.77	1.14	1.49	1.64	2.01	2.64	2.88	4.07	2.01	2.13	0.79	0.33	1.20
15	0.87	1.16	1.45	1.62	1.88	2.62	3.07	4.14	1.88	2.13	0.86	0.49	1.22
16	0.77	1.09	1.41	1.55	1.84	2.60	3.25	4.15	1.84	2.17	0.92	0.52	1.19
17	0.08	0.68	1.14	1.36	1.70	2.20	2.70	4.09	1.70	1.85	0.91	0.34	1.66
18	0.09	0.82	1.24	1.41	1.77	2.36	2.82	4.13	1.77	1.94	0.90	0.38	1.43
19	0.41	0.91	1.27	1.41	1.75	2.20	2.68	4.11	1.75	1.90	0.84	0.40	1.66
20	0.56	0.91	1.25	1.41	1.75	2.23	2.77	4.11	1.75	1.92	0.86	0.41	1.60
21	0.25	0.76	1.18	1.33	1.68	2.08	2.49	3.77	1.68	1.78	0.78	0.31	1.64
22	0.24	0.64	1.00	1.24	1.75	2.36	2.68	4.07	1.75	1.81	0.94	0.23	1.26
23	0.86	1.15	1.44	1.59	1.86	2.36	2.62	4.05	1.86	1.97	0.73	0.40	1.54
24	0.02	0.55	1.04	1.24	1.68	2.23	2.82	4.12	1.68	1.85	0.99	0.32	1.48
25	0.84	1.14	1.43	1.57	1.86	2.66	3.56	4.20	1.86	2.28	1.00	0.56	1.15
26	1.18	1.43	1.64	1.75	1.99	2.84	3.97	4.23	1.99	2.53	1.01	0.65	1.05
27	1.02	1.30	1.55	1.68	1.95	2.77	3.66	4.23	1.95	2.39	0.97	0.59	1.10
29	0.32	0.75	1.14	1.32	1.73	2.32	2.73	4.09	1.73	1.87	0.90	0.34	1.37
30	-0.94	-0.45	0.14	0.46	1.20	2.38	2.91	4.17	1.20	1.42	1.39	0.26	0.99
31	-1.37	-0.80	-0.23	0.06	0.68	1.41	1.82	3.86	0.68	0.76	1.22	0.24	1.41
32	0.82	1.14	1.43	1.59	1.88	2.50	2.84	4.12	1.88	2.05	0.80	0.43	1.34
33	0.19	0.59	0.95	1.14	1.55	1.97	2.64	4.14	1.55	1.71	0.96	0.37	1.75
34	0.68	1.14	1.41	1.57	1.86	2.64	4.00	4.23	1.86	2.42	1.12	0.59	1.18
35	0.36	0.97	1.30	1.48	1.89	2.75	4.00	4.24	1.89	2.40	1.17	0.50	1.06
36	-0.93	0.16	0.68	0.93	1.43	1.88	2.27	4.07	1.43	1.46	0.99	0.20	1.69
37	0.73	1.16	1.41	1.57	1.83	2.38	2.89	4.14	1.83	2.04	0.82	0.49	1.51
39	0.45	0.91	1.32	1.55	1.98	2.76	3.56	4.23	1.98	2.29	1.06	0.38	1.12
40	0.77	1.11	1.41	1.59	1.88	2.52	2.87	4.16	1.88	2.05	0.83	0.43	1.34
41	0.66	0.98	1.32	1.48	1.81	2.37	2.80	4.15	1.81	1.98	0.85	0.41	1.46
42	0.77	1.07	1.34	1.48	1.77	2.17	2.68	4.14	1.77	1.93	0.80	0.45	1.82
43	1.28	1.70	2.11	2.32	2.80	3.75	4.07	4.28	2.80	2.99	0.88	0.22	0.74
44	-0.59	0.23	0.60	0.80	1.19	1.64	1.82	3.35	1.19	1.20	0.78	0.21	1.52
45	0.04	0.51	0.95	1.14	1.56	1.93	2.41	4.09	1.56	1.64	0.91	0.29	1.86
46	0.34	0.68	0.99	1.18	1.56	1.93	2.32	4.07	1.56	1.62	0.85	0.31	1.85
47	-0.23	0.18	0.59	0.77	1.18	1.59	1.77	3.18	1.18	1.18	0.75	0.17	1.50
49	-1.30	0.00	0.41	0.59	1.02	1.55	1.77	4.00	1.02	1.07	0.95	0.30	1.71
50	-0.10	0.30	0.68	0.88	1.27	1.68	1.86	4.00	1.27	1.27	0.86	0.24	1.90
51	0.48	1.13	1.66	1.91	2.41	2.89	3.50	4.18	2.41	2.52	0.92	0.17	1.28
52	-0.34	0.30	0.75	0.95	1.34	1.73	1.91	3.77	1.34	1.33	0.82	0.19	1.82
53	-1.38	0.09	0.48	0.67	1.09	1.59	1.82	3.23	1.09	1.13	0.81	0.23	1.40
54	0.42	0.80	1.14	1.28	1.62	1.94	2.22	3.41	1.62	1.66	0.67	0.24	1.62

Table 3.1 *(Continued)*: Phi (Φ) values and computed grain size parameters for the studied sandstone samples.

S. No.	Φ1	Φ5	Φ16	Φ25	Φ50	Φ75	Φ84	Φ95	Md	Mz	σ_I	Sk_I	K_G
55	-0.25	0.64	1.16	1.32	1.64	1.95	2.27	4.03	1.64	1.69	0.79	0.27	2.21
56	-0.38	0.34	0.74	0.94	1.43	1.93	2.36	4.05	1.43	1.51	0.97	0.28	1.54
57	-1.45	0.14	0.67	0.94	1.36	1.77	1.95	2.88	1.36	1.33	0.74	0.02	1.35
58	0.98	1.23	1.49	1.60	1.84	2.23	2.54	4.01	1.84	1.96	0.68	0.45	1.81
59	0.64	1.13	1.45	1.60	1.93	2.41	2.68	4.06	1.93	2.02	0.75	0.34	1.48
60	0.66	1.05	1.42	1.62	2.00	2.77	3.32	4.18	2.00	2.25	0.95	0.39	1.12
61	0.36	0.91	1.62	1.95	2.49	2.99	3.82	4.23	2.49	2.64	1.05	0.13	1.31
62	-1.18	-0.35	0.27	0.50	0.98	1.68	2.00	3.91	0.98	1.08	1.08	0.28	1.48
63	0.20	0.68	1.10	1.28	1.68	2.14	2.50	4.05	1.68	1.76	0.86	0.29	1.61
64	0.21	0.77	1.25	1.45	1.89	2.55	2.86	4.14	1.89	2.00	0.91	0.27	1.26
65	1.05	1.36	1.59	1.72	1.98	2.56	2.86	4.14	1.98	2.14	0.74	0.47	1.36
66	0.18	0.66	1.09	1.23	1.55	1.82	1.97	3.84	1.55	1.54	0.70	0.20	2.21
67	0.89	1.15	1.37	1.50	1.76	2.00	2.43	4.06	1.76	1.85	0.71	0.42	2.39
68	0.85	1.19	1.46	1.59	1.85	2.36	2.80	4.15	1.85	2.04	0.78	0.49	1.58
69	-0.01	0.30	0.59	0.73	1.05	1.55	1.80	4.03	1.05	1.15	0.87	0.42	1.86
70	-0.25	0.15	0.77	1.12	1.77	2.59	3.05	4.17	1.77	1.86	1.18	0.16	1.12
71	-0.27	0.23	0.57	0.73	1.13	1.64	1.86	3.68	1.13	1.19	0.85	0.31	1.55
72	-0.45	0.21	0.64	0.85	1.26	1.67	1.86	2.99	1.26	1.25	0.73	0.11	1.39
73	-1.66	-0.58	0.23	0.48	1.02	1.50	1.70	2.58	1.02	0.98	0.85	-0.04	1.27
74	-1.18	-0.45	0.20	0.48	1.09	1.73	2.00	4.02	1.09	1.10	1.13	0.16	1.47
75	0.14	0.41	0.68	0.82	1.18	1.64	1.86	3.10	1.18	1.24	0.70	0.29	1.34
76	0.36	0.64	0.90	1.04	1.43	1.84	2.17	4.09	1.43	1.50	0.84	0.35	1.77
77	-0.70	0.36	0.80	1.00	1.38	1.77	1.93	3.82	1.38	1.37	0.81	0.19	1.84
78	0.14	0.63	1.08	1.25	1.63	2.00	2.73	4.02	1.63	1.69	0.84	0.28	1.85
79	-2.62	-1.68	-0.79	-0.35	0.39	1.04	1.44	3.09	0.39	0.35	1.28	0.04	1.41
80	-0.36	0.52	1.08	1.24	1.59	1.91	2.18	3.45	1.59	1.62	0.72	0.17	1.79
81	0.18	0.51	0.82	0.96	1.34	1.73	1.91	2.95	1.34	1.36	0.64	0.18	1.30
82	0.18	0.55	0.90	1.05	1.39	1.73	1.86	2.74	1.39	1.38	0.57	0.11	1.32
83	-0.95	0.00	0.42	0.64	1.09	1.54	1.73	2.75	1.09	1.08	0.74	0.09	1.25
84	0.68	0.99	1.27	1.41	1.73	2.06	2.45	4.04	1.73	1.82	0.76	0.37	1.92
85	-1.09	-0.43	0.09	0.27	0.63	0.98	1.26	1.92	0.63	0.66	0.65	0.09	1.36
86	0.39	0.81	1.14	1.25	1.54	1.78	1.91	3.41	1.54	1.53	0.59	0.20	2.01
87	—	0.69	1.36	1.55	1.93	2.64	2.96	4.14	1.93	2.08	0.92	0.28	1.30
90	0.23	0.58	0.89	1.06	1.43	1.80	1.95	4.00	1.43	1.42	0.78	0.24	1.89
91	0.28	0.56	0.82	0.94	1.27	1.61	1.77	2.66	1.27	1.29	0.56	0.19	1.28
92	-0.09	0.18	0.45	0.58	0.85	1.25	1.50	2.11	0.85	0.93	0.55	0.27	1.18
93	0.00	0.36	0.72	0.89	1.25	1.61	1.77	2.50	1.25	1.25	0.59	0.08	1.22
94	-1.75	-0.65	0.23	0.47	1.05	1.59	1.84	2.96	1.05	1.04	0.95	0.02	1.32
95	-0.60	0.09	0.55	0.77	1.20	1.61	1.80	3.06	1.20	1.18	0.76	0.11	1.45
96	-0.77	0.27	1.07	1.20	1.50	1.78	1.91	2.98	1.50	1.49	0.62	0.03	1.91
97	-0.74	0.36	0.94	1.16	1.58	1.99	2.32	3.52	1.58	1.61	0.82	0.15	1.56
98	1.20	1.52	1.80	1.93	2.32	2.73	2.91	4.12	2.32	2.34	0.67	0.22	1.33
99	-1.23	-0.09	0.41	0.64	1.13	1.68	1.92	4.07	1.13	1.15	1.01	0.23	1.64
100	-0.17	0.36	0.77	0.96	1.35	1.73	1.91	3.77	1.35	1.34	0.80	0.20	1.81
101	0.12	0.59	1.02	1.18	1.50	1.82	1.95	3.84	1.50	1.49	0.72	0.20	2.08
102	0.23	0.66	1.05	1.18	1.50	1.77	1.91	3.25	1.50	1.49	0.61	0.15	1.80
103	0.33	0.58	0.84	0.96	1.42	1.91	2.30	4.05	1.42	1.52	0.89	0.36	1.50
104	0.11	0.40	0.68	0.82	1.14	1.52	1.68	2.18	1.14	1.17	0.52	0.12	1.04
105	-2.71	-1.76	-0.86	-0.41	0.34	0.91	1.28	3.00	0.34	0.25	1.26	0.00	1.48
107	-2.62	-1.65	-0.76	-0.32	0.41	1.11	1.79	2.85	0.41	0.48	1.32	0.08	1.29
108	-0.84	0.52	1.08	1.26	1.64	2.05	2.31	2.85	1.64	1.68	0.66	0.06	1.21
110	-0.20	0.32	0.74	0.95	1.35	1.74	1.92	2.73	1.35	1.34	0.66	0.06	1.25
111	0.33	0.68	1.00	1.16	1.48	1.78	1.92	2.40	1.48	1.47	0.49	0.01	1.14
Max	1.28	1.70	2.11	2.32	2.80	3.75	4.07	4.28	2.80	2.99	1.39	0.65	2.39
Min	-2.71	-1.76	-0.86	-0.41	0.34	0.91	1.26	1.92	0.34	0.25	0.49	-0.04	0.74
Avg	-0.04	0.53	0.95	1.14	1.53	2.04	2.41	3.70	1.53	1.63	0.85	0.27	1.49

Md = Median Mz = Graphic mean size σ_I = Standard deviation

Sk_I = Skewness K_G = Kurtosis

Table 3.2: Summery of the computed grain size parameters for the studied sandstone samples.

Parameter		Araba Formation		Naqus Formation	
		Φ	Description	Φ	Description
Median (Md)					
	Range	2.38 - 3.59	V.F - F	0.34 - 2.80	F - C
	Average	2.86	F	1.53	M
	Variance	0.13		0.19	
Graphic Mean (Mz)					
	Range	2.54 - 3.29	V.F - F	0.25 - 2.99	F - C
	Average	2.95	F	1.63	M
	Variance	0.06		0.26	
Standard Deviation (σ_I)					
	Range	0.64 - 1.03	MWS - PS	0.49 - 1.39	WS -PS
	Average	0.85	MS	0.85	MS
	Variance	0.02		0.03	
Skewness (Sk_I)					
	Range	-0.45 - 0.43	SCS - SFS	-0.04 - 0.65	NS -SFS
	Average	0.12	FS	0.27	FS
	Variance	0.05		0.02	
Kurtosis (K_G)					
	Range	0.66 - 1.15	VPK -LK	0.74 - 2.39	PK - VLK
	Average	0.84	PK	1.49	LK
	Variance	0.02		0.09	

C = Coarse Grained
M = Medium Grained
F = Fine Grained
V.F = Very Fine Grained

WS = Well Sorted
MWS = Moderately Well Sorted
MS = Moderately Sorted
PS = Poorly Sorted

SCS = Strongly Coarse Skewed
NS = Nearly Symmetrical
FS = Fine Skewed
SFS = Strongly Fine Skewed

VPK = Very Platykurtic
PK = Platykurtic
LK = Leptokurtic
VLK = Very Leptokurtic

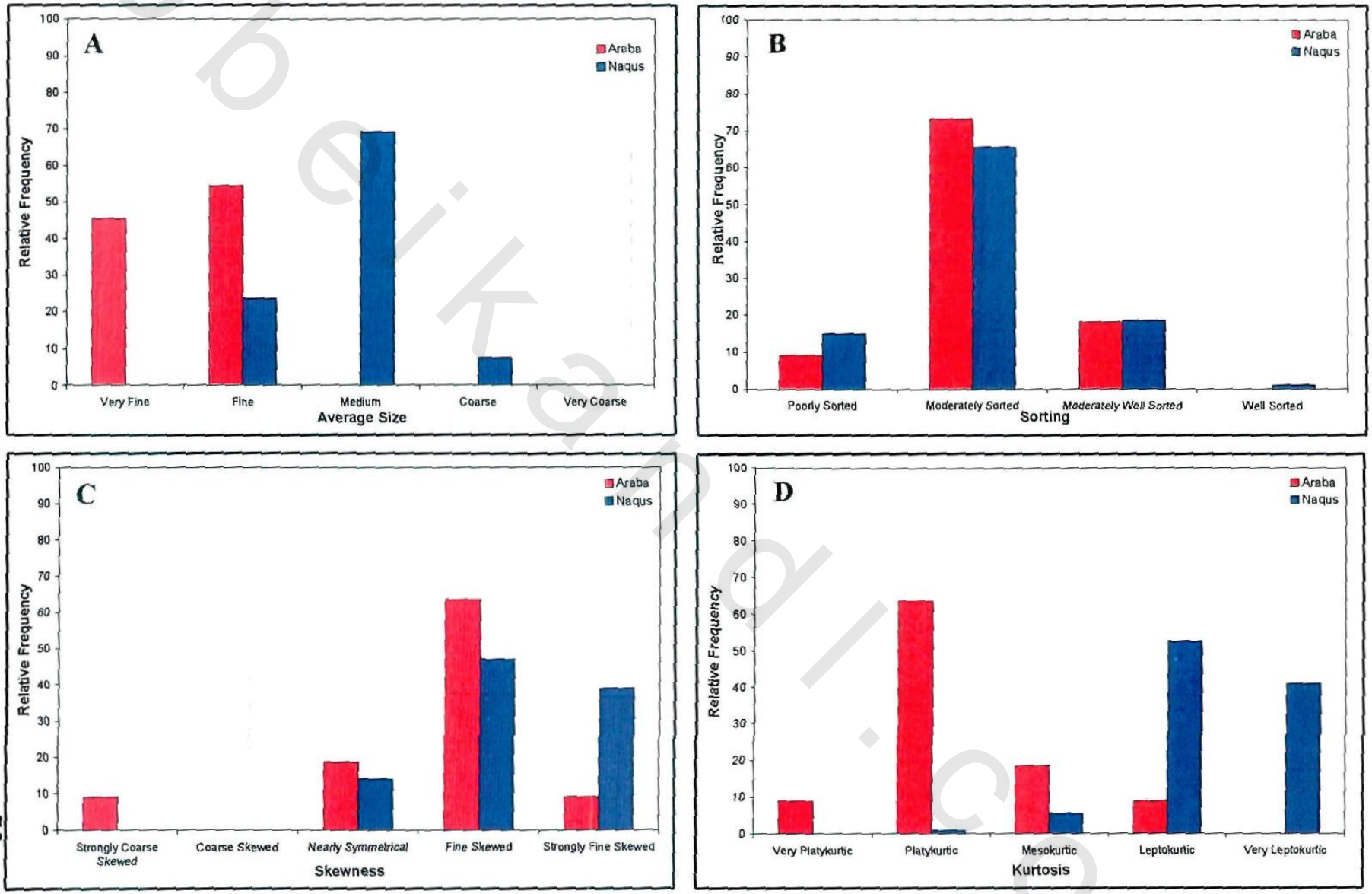

Fig. 3.3: Frequency distribution of average grain size (A), sorting (B), skewness (C) and kurtosis (D) for Araba and Naqus sandstones.

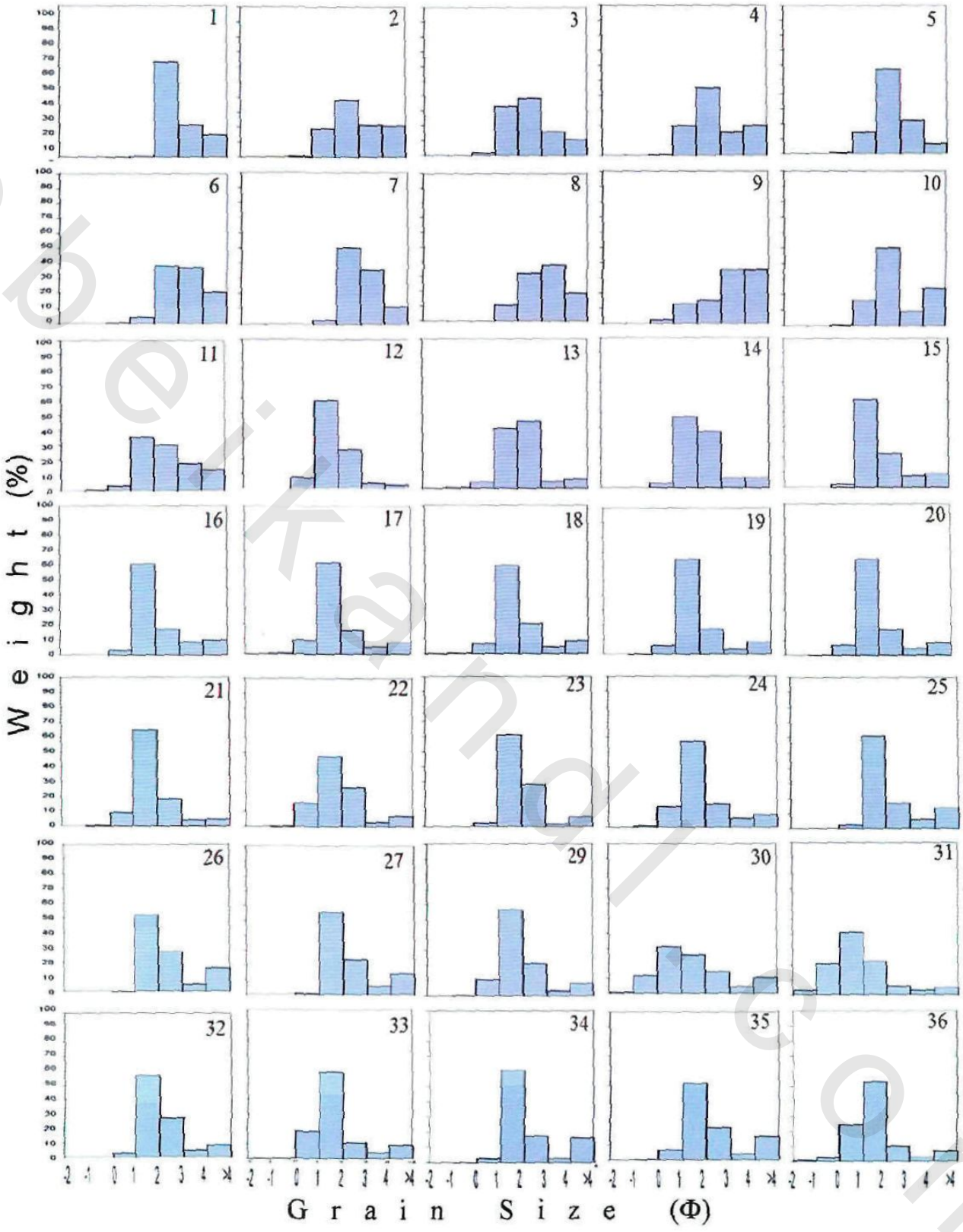

Fig. 3.4: Histograms of grain size distribution for Araba (1-11) and Naqus (12-36) sandstoness.

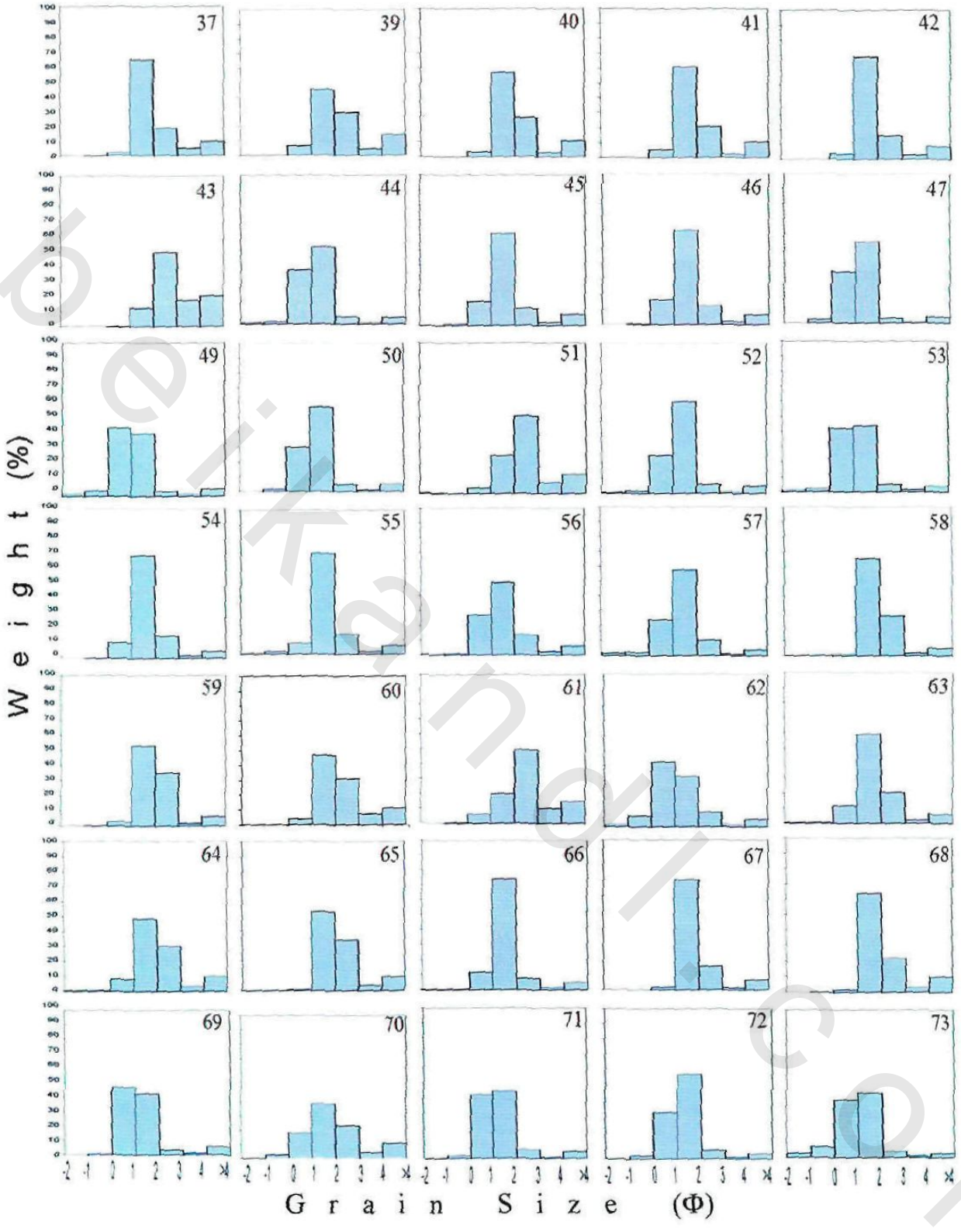

Fig. 3.4 *(Continued)*: Histograms of grain size distribution for Naqus Sandstone.

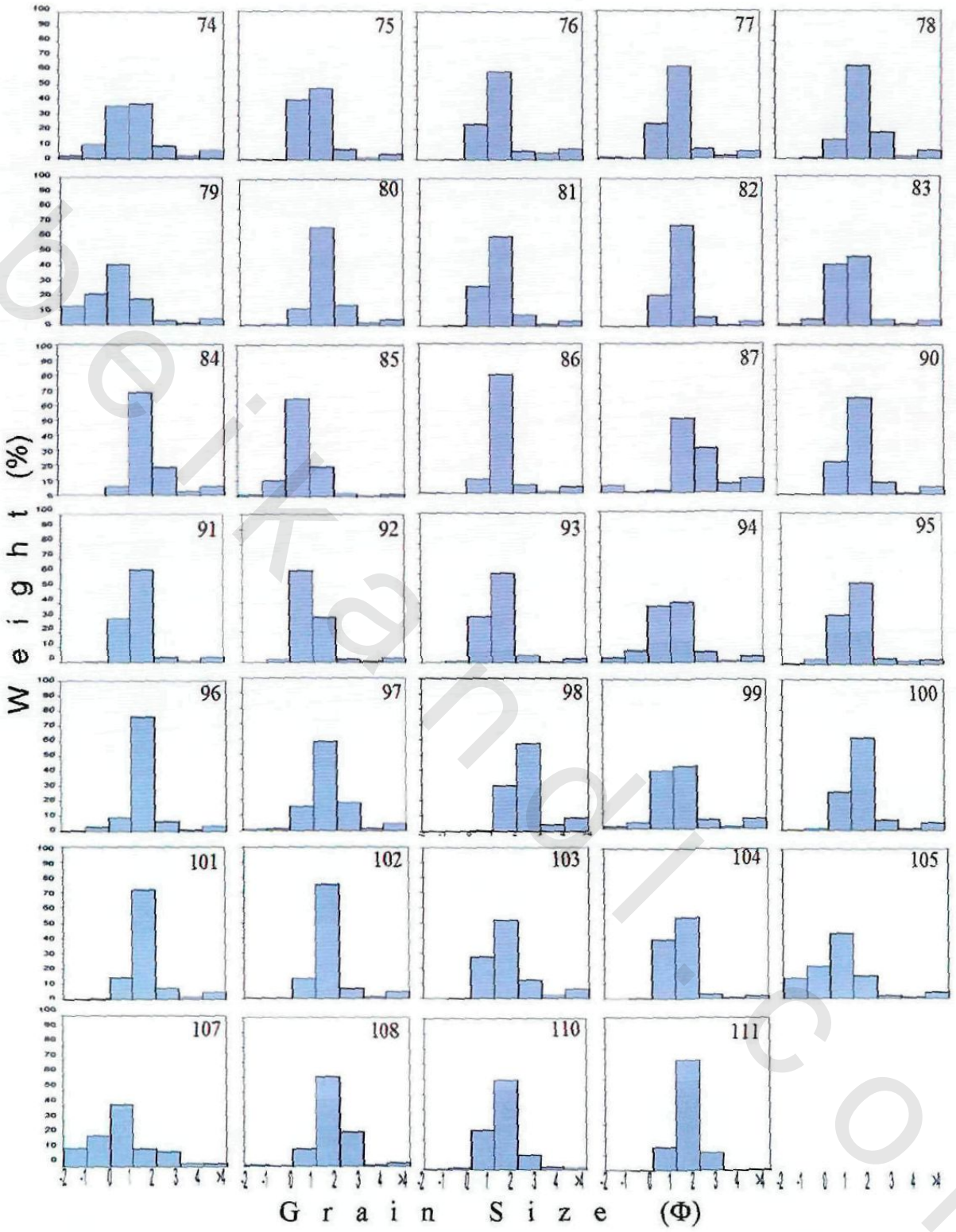

Fig. 3.4 *(Continued)*: Histograms of grain size distribution for Naqus sandstone.

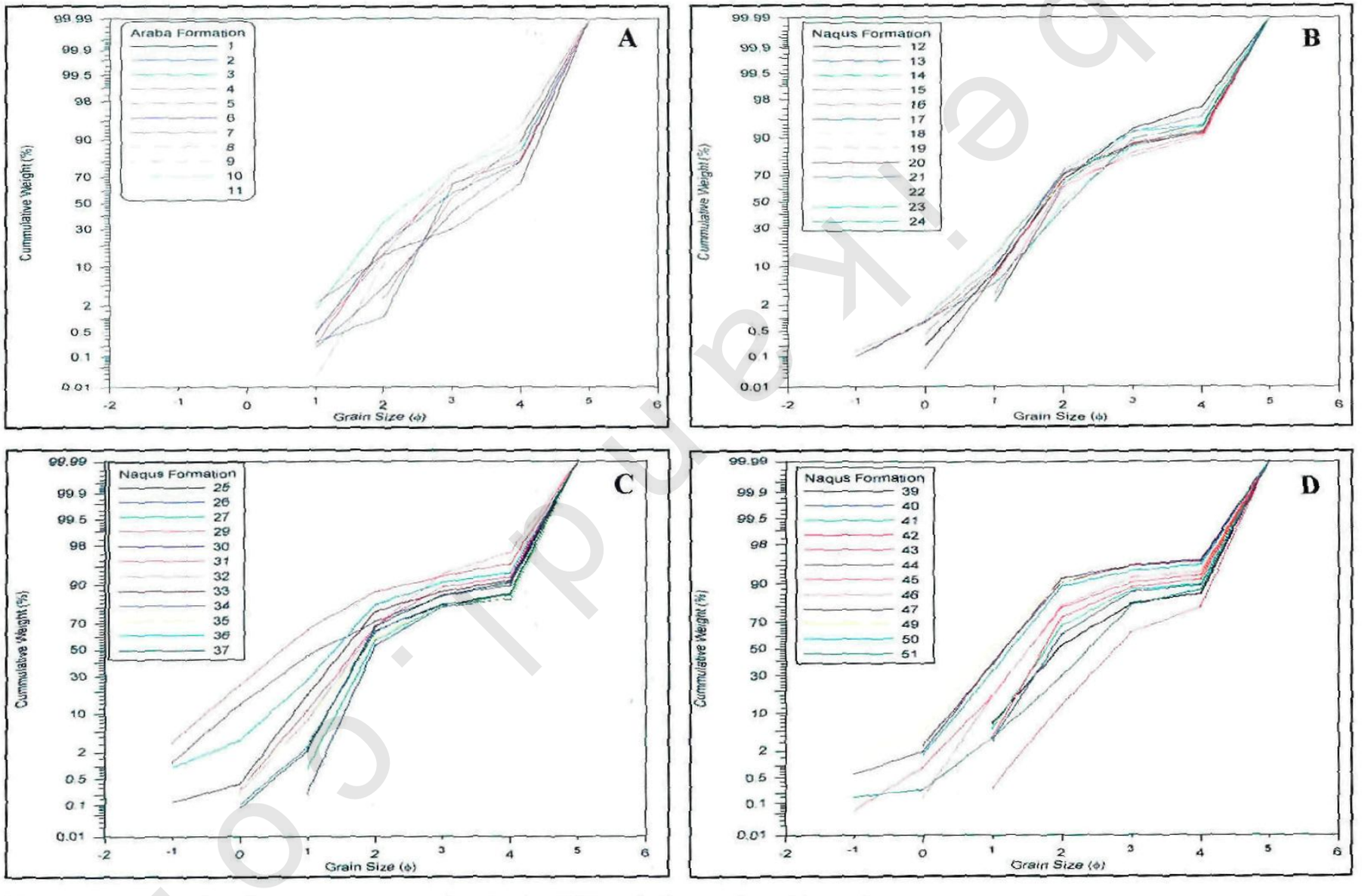

Fig. 3.5: Cumulative frequency curves for Araba (A) and Naqus (B - D) sandstones.

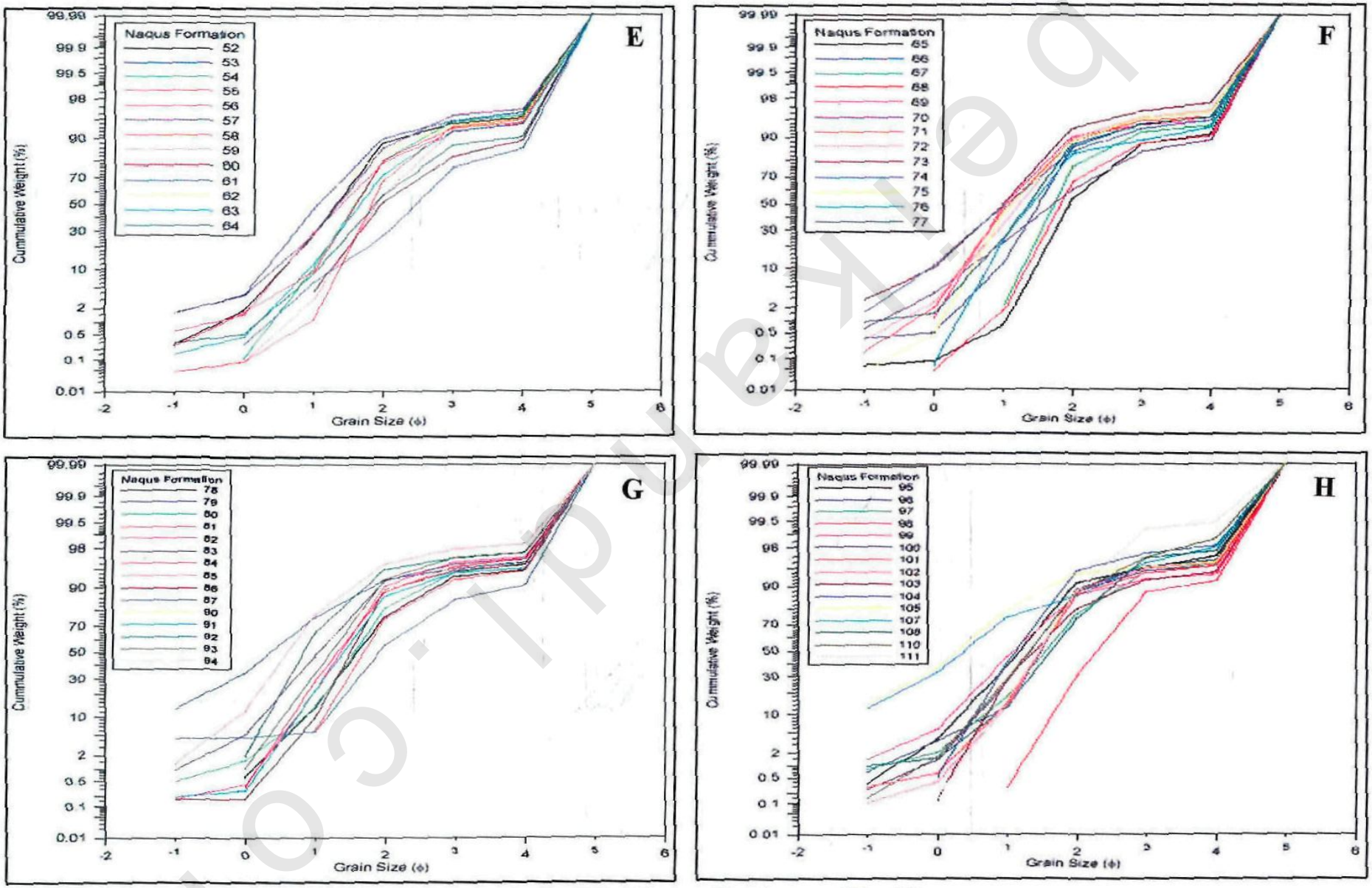

Fig. 3.5 *(Contimued)*: Cumulative frequency curves for Naqus Sandstone (E – H).

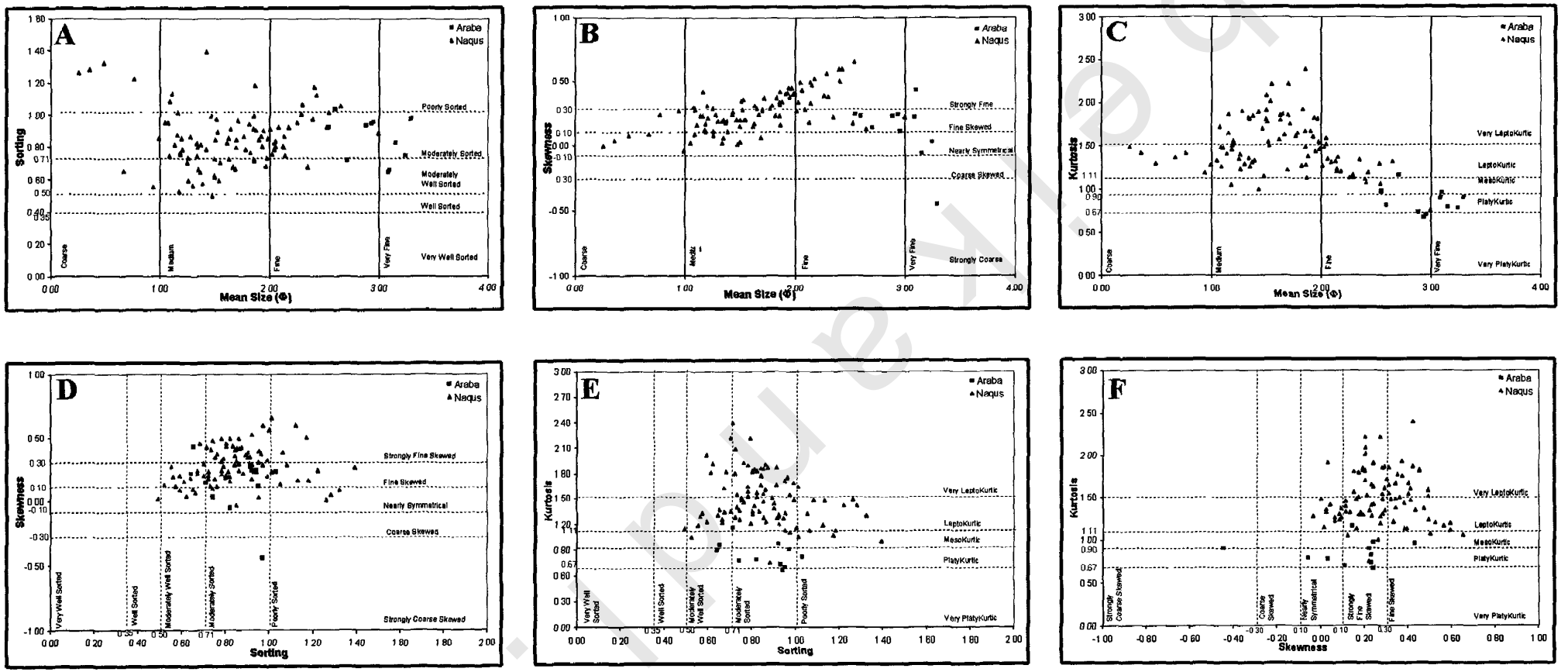

Fig. 3.6: Cross plot diagrams of different size parameters for Araba and Naqus sandstones: mean size versus sorting (A), mean size versus skewness (B), mean size versus kurtosis (C), sorting versus skewness (D), sorting versus kurtosis (E) and skewness versus kurtosis (F).

3.3.1 Histograms

In Naqus Formation, the "two bars" histograms are the most common. The next abundant type is that in which the majority of the distribution falls in three or more size grades. Another less abundant type is the "one bar" histogram in which more than 65 % of the sample belongs to one size grade. The observed unimodality of the studied samples may be attributed to their inheritance from the same provenance and may indicate a fluvial origin. On the other hand, the two bars distribution pattern indicates the great influence of the hydrodynamic action of the transporting agent and/or the depositing media.

In Araba Formation, two more or less types of distribution are observed. The most common type is the one in which the majority of the distribution falls in three or more size grades. The other common distribution is the "two bars" histograms in which more than 80 % of the sample is distributed between two consecutive size grades.

3.3.2 Cumulative frequency curves

Frequency curves (Fig. 3.5) were constructed to show the percent of grains coarser or finer than any given grain size for an individual sample.

3.3.3 Average size

Average size is defined by a variety of statistical parameters. Simplest of which are the median and the mean. The median diameter ranges from 0.34 to 2.8 ϕ (fine to coarse) with an average of 1.53 ϕ (medium) in Naqus Formation and from 2.38 to 3.59 ϕ (very fine to fine) with an average of 2.86 ϕ (fine) in Araba Formation. In Naqus Formation, graphic mean size (Mz) ranges from 0.25 to 2.99 ϕ (fine to coarse) with an average of 1.63 ϕ (medium). It fluctuates frequently reflecting the change of the competency of the depositing medium. 23.5 % of the samples are fine grained, 69 % are medium grained and 7.5 % are coarse grained (Fig.

3.3A). On the other hand, the graphic mean size (Mz) in Araba Formation ranges from 2.54 to 3.29 ϕ (very fine to fine) with an average of 2.95 ϕ (fine), indicating that the studied sediments are limited within a small range of sand sizes. 45.5 % of the samples are very fine grained and 54.5 % are fine grained (Fig. 3.3A).

3.3.4 Standard deviation

In Naqus Formation, the standard deviation values range from 0.49 ϕ to 1.39 ϕ (well sorted to poorly sorted) with an average of 0.85 ϕ (moderately sorted). 15 % of the samples are poorly sorted, 65.5 % are moderately sorted, 18.5 % are moderately well sorted and 1 % is well sorted (Fig. 3.3B). On the other hand, standard deviation values in Araba Formation range from 0.64 to 1.03 ϕ (moderately well sorted to poorly sorted) with an average of 0.85 ϕ (moderately sorted). 9 % of the samples are poorly sorted, 73 % are moderately sorted and 18 % are moderately well sorted (Fig. 3.3B).

3.3.5 Skewness

In Naqus Formation, the skewness values range from -0.04 ϕ (nearly symmetrical) to 0.65 ϕ (strongly fine skewed) with an average of 0.27 ϕ (fine skewed). 14 % of the samples are nearly symmetric, 47 % are fine skewed and 39 % are strongly fine skewed (Fig. 3.3C). The studied samples of Araba Formation have skewness values that range from -0.45 ϕ (strongly coarse skewed) to 0.43 ϕ (strongly fine skewed) with an average of 0.12 ϕ (fine skewed). 9 % of the samples are strongly coarse skewed, 18.5 % are nearly symmetric, 63.5 % are fine skewed and 9 % are strongly fine skewed (Fig. 3.3C).

3.3.6 Kurtosis

In Naqus Formation, kurtosis ranges from 0.74 ϕ (platykurtic) to 2.39 ϕ (very leptokurtic) with an average of 1.49 ϕ (leptokurtic). 1 % of the

samples are platykurtic, 5.5 % are mesokurtic, 52.5 % are leptokurtic and 41 % are very leptokurtic (Fig. 3.3D). They indicate that the central portions of the grain size distribution curves are better sorted than the tails. Kurtosis values in Araba Formation range from 0.66 ϕ (very platykurtic) to 1.15 ϕ (leptokurtic) with an average of 0.84 ϕ (platykurtic). 9 % of the samples are very platykurtic, 63.5 % are platykurtic, 18.5 % are mesokurtic and 9 % are leptokurtic (Fig. 3.3D). They indicate that the tails of the grain size distribution curves are better sorted than the central portions mostly due to the addition of some silt matrix, or the central portions and the tails are almost equally sorted.

3.3.7 Bivariate relationships of grain size parameters

3.3.7.1 Mean size versus standard deviation

No particular correlation was found between these two parameters in Naqus Formation. However, samples with medium size have better sorting than those of coarse and fine sizes (Fig. 3.6A). On the other hand, plot of mean size versus standard deviation for Araba Formation shows a slight negative correlation indicating that decrease of mean size is associated with slightly better sorting (Fig. 3.6A). The slight negative correlation may be attributed to a unidirectional environment.

3.3.7.2 Mean size versus skewness

In Naqus Formation, crossplot of mean size versus skewness shows a moderate positive correlation. The coarse grained sediments are nearly symmetrical or positive skewed. Sediments with medium grain diameter are positive and/or strongly positive skewed with few nearly symmetrical. Fine grained sediments are mostly strongly positive skewed with some positive. Overall, with the decrease in mean grain diameter, the skewnesses of the sediments become more positively skewed which could be attributed to the addition of finer materials (Fig. 3.6B). Such behavior

may support the idea of unidirectional depositional currents. Plot of mean size versus skewness in Araba Formation indicates that sediments with fine grain diameter are fine skewed, while those with very fine grain diameter have a wide range of skewnesses (strongly coarse skewed to strongly fine skewed). Moderate negative correlation exists between the two parameters (Fig. 3.6B).

3.3.7.3 Mean size versus kurtosis

No particular correlation was found between these two parameters in Naqus Formation. The samples are generally mesokurtic to very leptokurtic with the dominance of leptokurtosis (Fig. 3.6C). The leptokurtic character showing better sorting in the central portion of the distribution than in the tails, may correspond to what Mason and Folk (1958) termed "aeolian flat". This term is not meant that these sediments are deposited by aeolian agent but signifies that the present day skin of the sediments is influenced by wind action (cf. El-Hinnawi et al., 1973). This explains the more pronounced leptokurtic character of the present samples. However, with the decrease in mean grain diameter (fine sediments), the sorting of the tails becomes better. In Araba Formation, plots of the studied samples show platylurtic to mesokurtic characters, which indicate that the tails of the grain size distribution curves are better sorted than the central portions mostly due to the addition of some silt matrix, or the central portions and the tails are almost equally sorted (Fig. 3.6C).

3.3.7.4 Sorting versus skewness

The scatter plot diagrams of standard deviation against skewness (in both Naqus and Araba formations) show that sorting is more or less the same in all the symmetry classes. However, the better the sorting, the smaller the fluctuation of the sediments' skewness (Fig. 3.6D).

3.3.7.5 Sorting versus kurtosis

In Naqus Formation, leptokurtosis is associated with better sorting. On the other hand, no particular correlation was found between the two parameters in Araba Formation. (Fig. 3.6E).

3.3.7.6 Skewness versus kurtosis

In Naqus Formation, leptokurtosis is associated with finer skewness. On the other hand, no particular correlation was found between the two parameters in Araba Formation (Fig. 3.6F).

Plate 3.1

A) Varicolored (1, 2, 3, 4), channel fill, fine grained sandstone. Araba Formation.

B) Varicolored laminated sandstone. Araba Formation.

C, D) Thin layers of red and yellow iron minerals. Calcite-cemented sandstone pebbles are observed near the topmost part. Yellowish streaks of clay materials are also present. Desert varnish is observed at the upper part of the formation. Araba Formation.

Plate 3.1

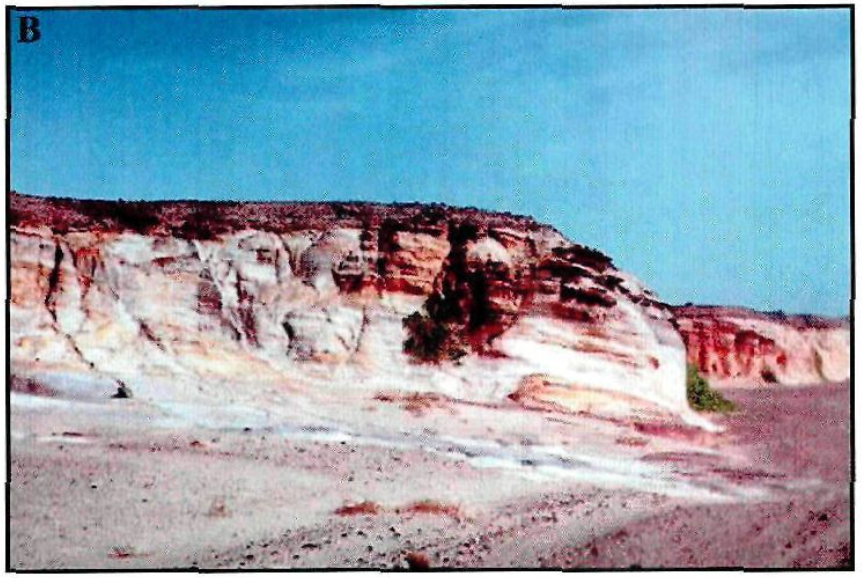

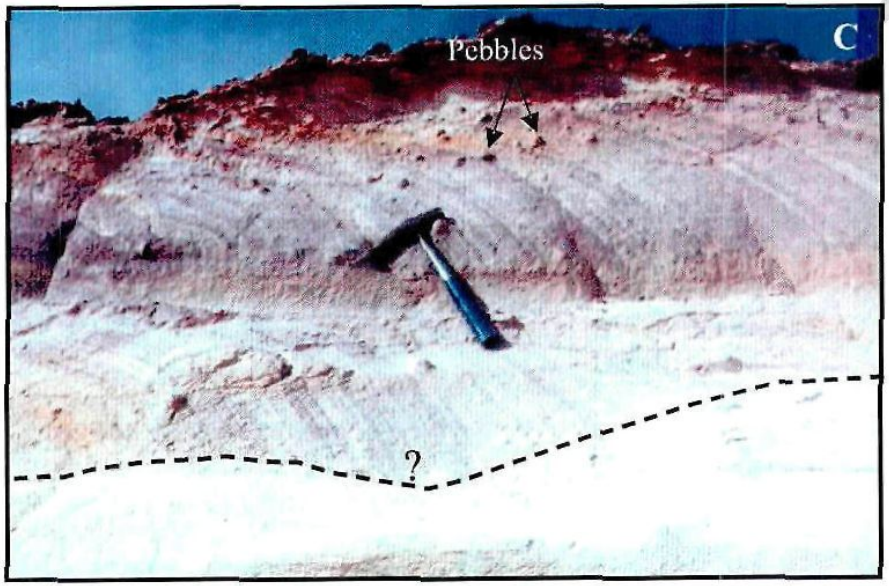

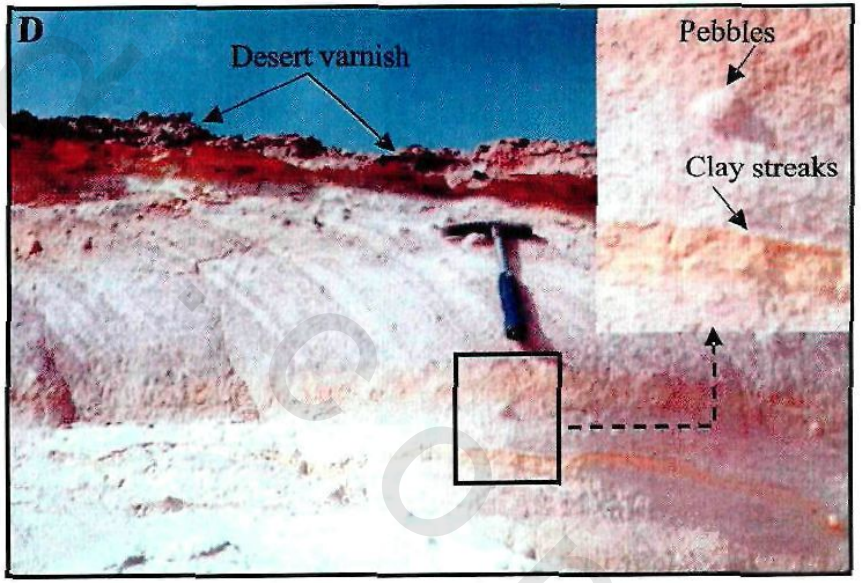

Plate 3.2

A) Color mottling and planar lamination. Araba Formation.

B) Burrowing organisms (Skolithos tubes) penetrating the beds for several centimeters. Araba Formation.

C) Quartz pebbles and cobbles along the foreset lamina. Naqus Formation.

D) Randomly distributed quartz pebbles and cobbles. Naqus Formation.

Plate 3.2

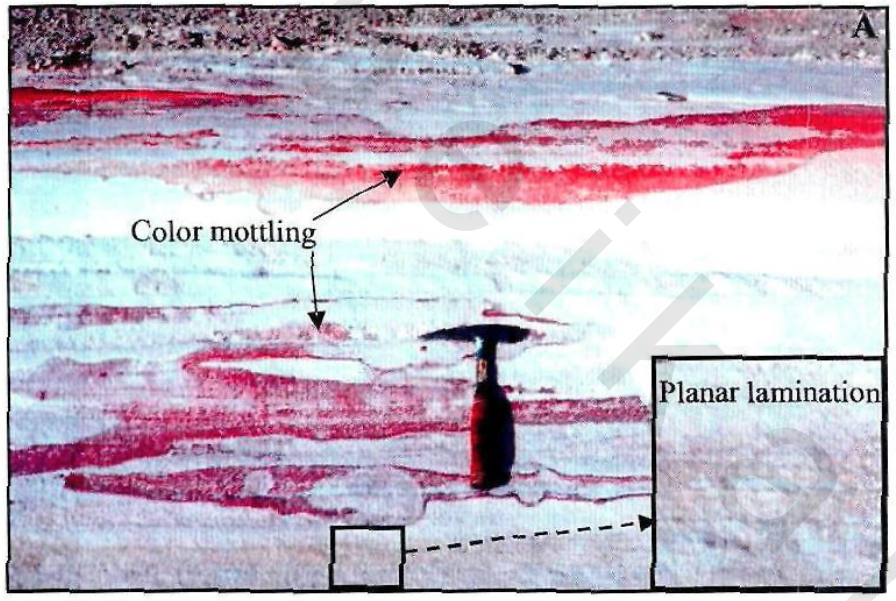
A
Color mottling
Planar lamination

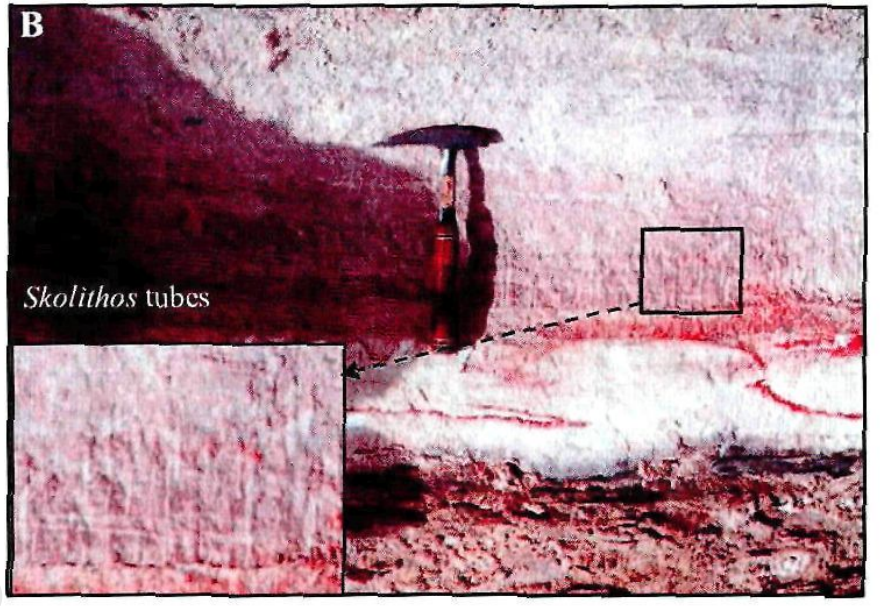
B
Skolithos tubes

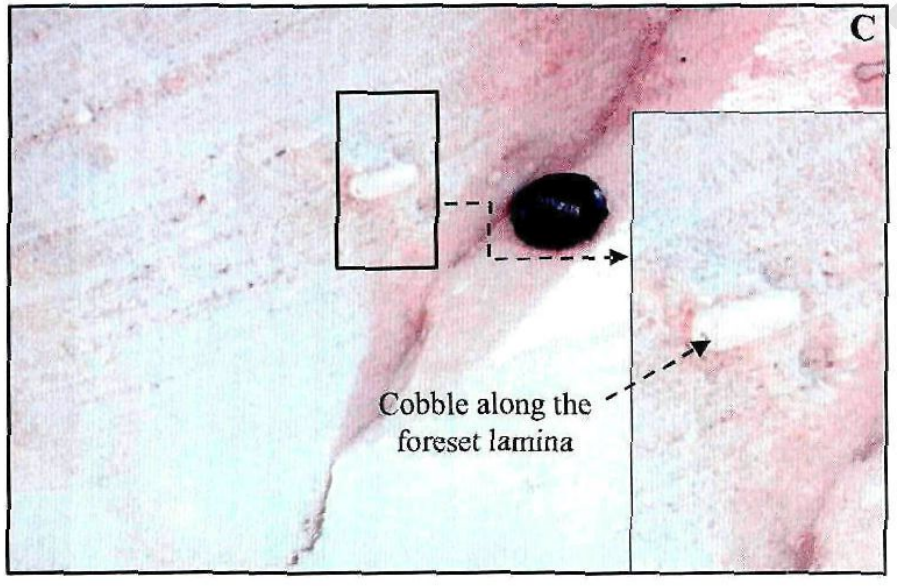
C
Cobble along the
foreset lamina

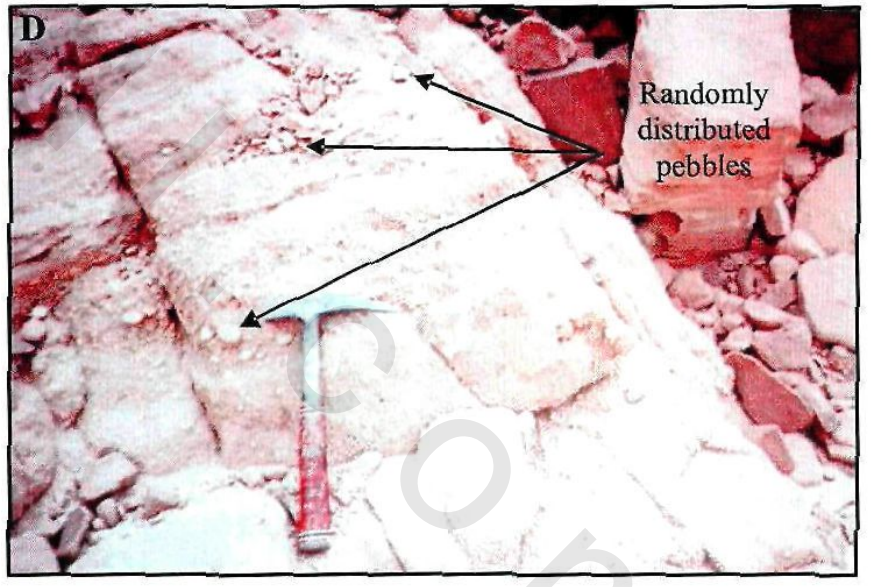
D
Randomly
distributed
pebbles

Plate 3.3

A, B) Highly jointed, silica-cemented sandstone of limited extension (silcrete). Most of the joints are oblique, vertical and open; some are filled by calcite and/or gypsum. Topmost part of the Naqus Formation.

C) An igneous dyke cutting through the Early Paleozoic Naqus Sandstone. Note the differential weathering due to wind action. Naqus Formation.

D) Sandstone/quartizite, white, hard, well cemented, apparently massive, with abundant fractures. Scattered large quartz grains have a just discernible orientation, which suggests a possible dip of 45° for this massive sandstone. RB-A1 well, depth 12465.50-12466.00 ft.

E) Breccia, polymictic with green sandstone matrix that includes white sandstone blocks and clasts and angular red claystone clasts. Fractured, possibly the result of core handling. RB-A1 well, depth 12347.00-12348.00 ft.

Plate 3.3

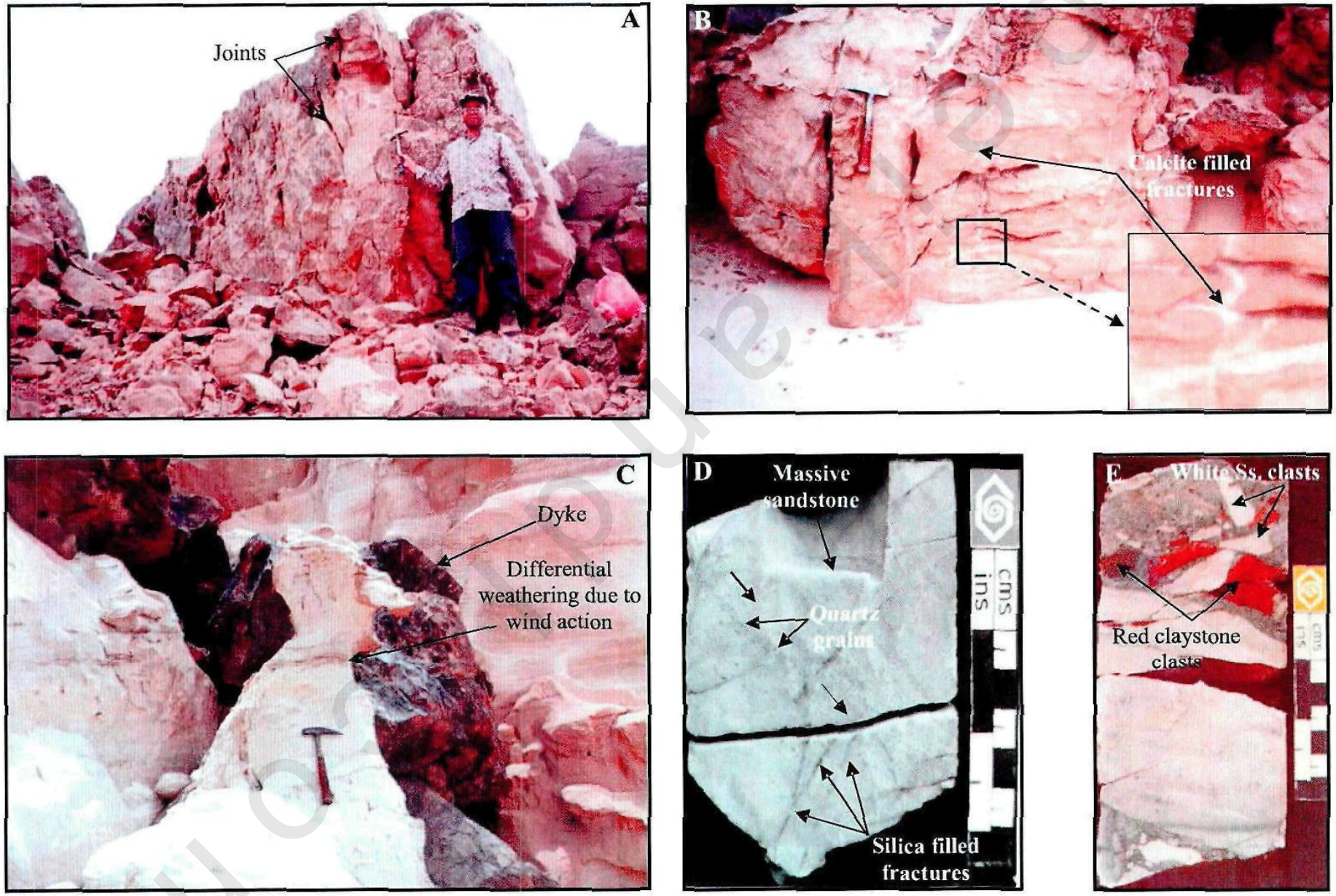
A
Joints
B
Calcite filled fractures
C
Dyke
Differential weathering due to wind action
D
Massive sandstone
Quartz grains
Silica filled fractures
cms
ins
E
White Ss. clasts
Red claystone clasts

Plate 3.4

A) Fractured white sandstone masses up to 2 feet in diameter. Photograph shows base of mass in green sandstone. Derived block intensely fractured, but fractures cemented with siliceous cement. RB-A1 well, depth 12346.00-12347.00 ft.

B) Sandstone, white and light green, heavily bituminous where porous, bimodal grain distribution, generally medium to coarse with granules and clasts. Fractures are partially filled with siliceous cement. RB-A1 well, depth 12336.00-12337.00 ft.

C) Sandstone, white and light green, massive, porous, heavily oil stained, with scattered quartz and lithic granules. High angle open fractures. RB-A1 well, depth 12340.00-12341.00 ft.

Plate 3.4

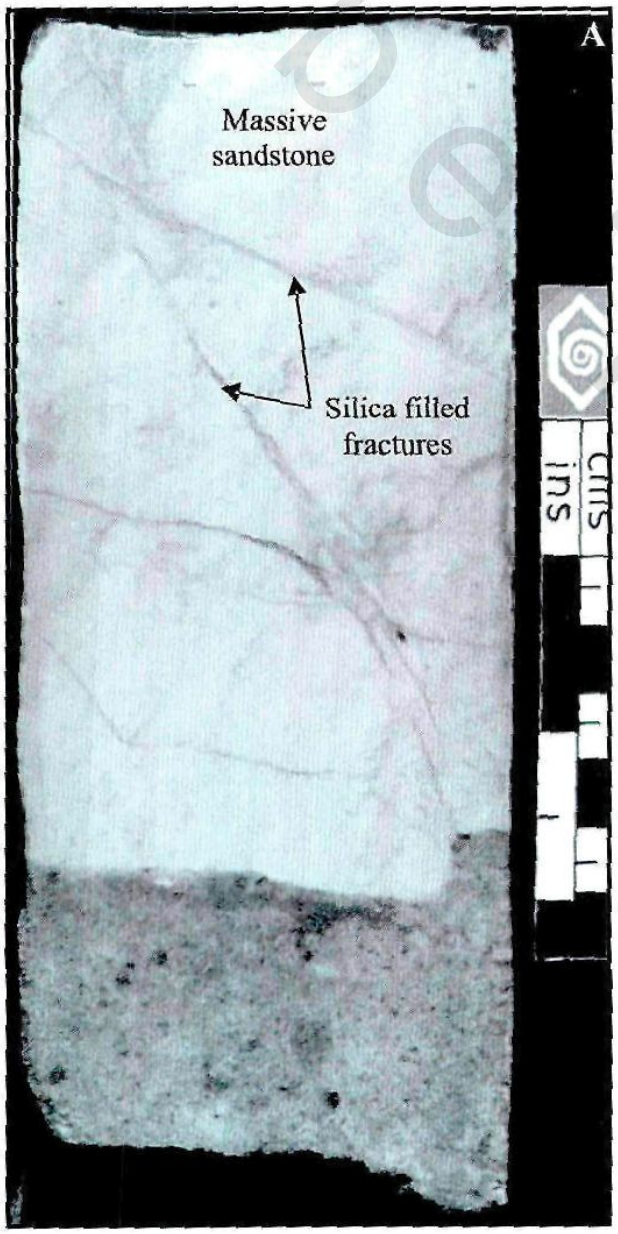
A
Massive sandstone
Silica filled fractures
cms
ins

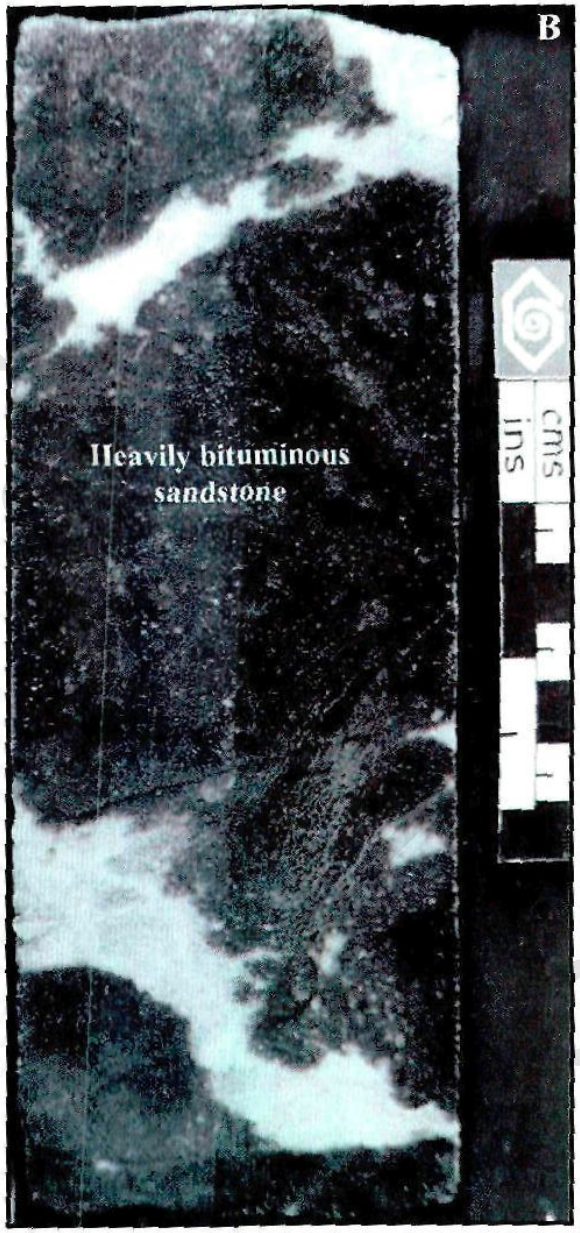
B
Heavily bituminous sandstone
cms
ins

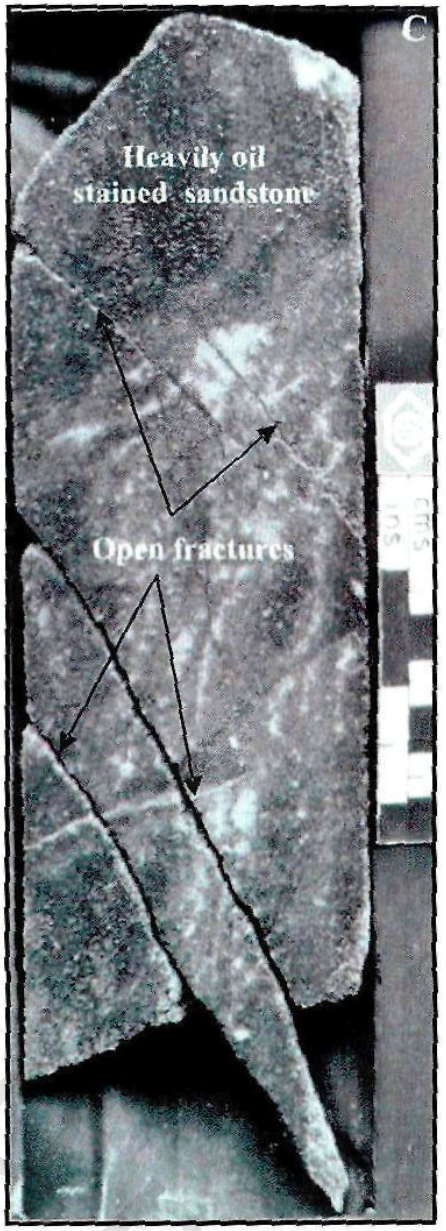
C
Heavily oil stained sandstone
Open fractures

Plate 3.5

A) Bioturbation. RB-B7 well, depth 12274.85-12276.10 ft.

B) Bioturbation. RB-C2 well, depth 12320.55-12320.95 ft.

C) Enlargement of B.

D) Channel structure filled by fine grained, planar laminated sandstone The sandstone was later subjected to coloration. Araba Formation.

Plate 3.5

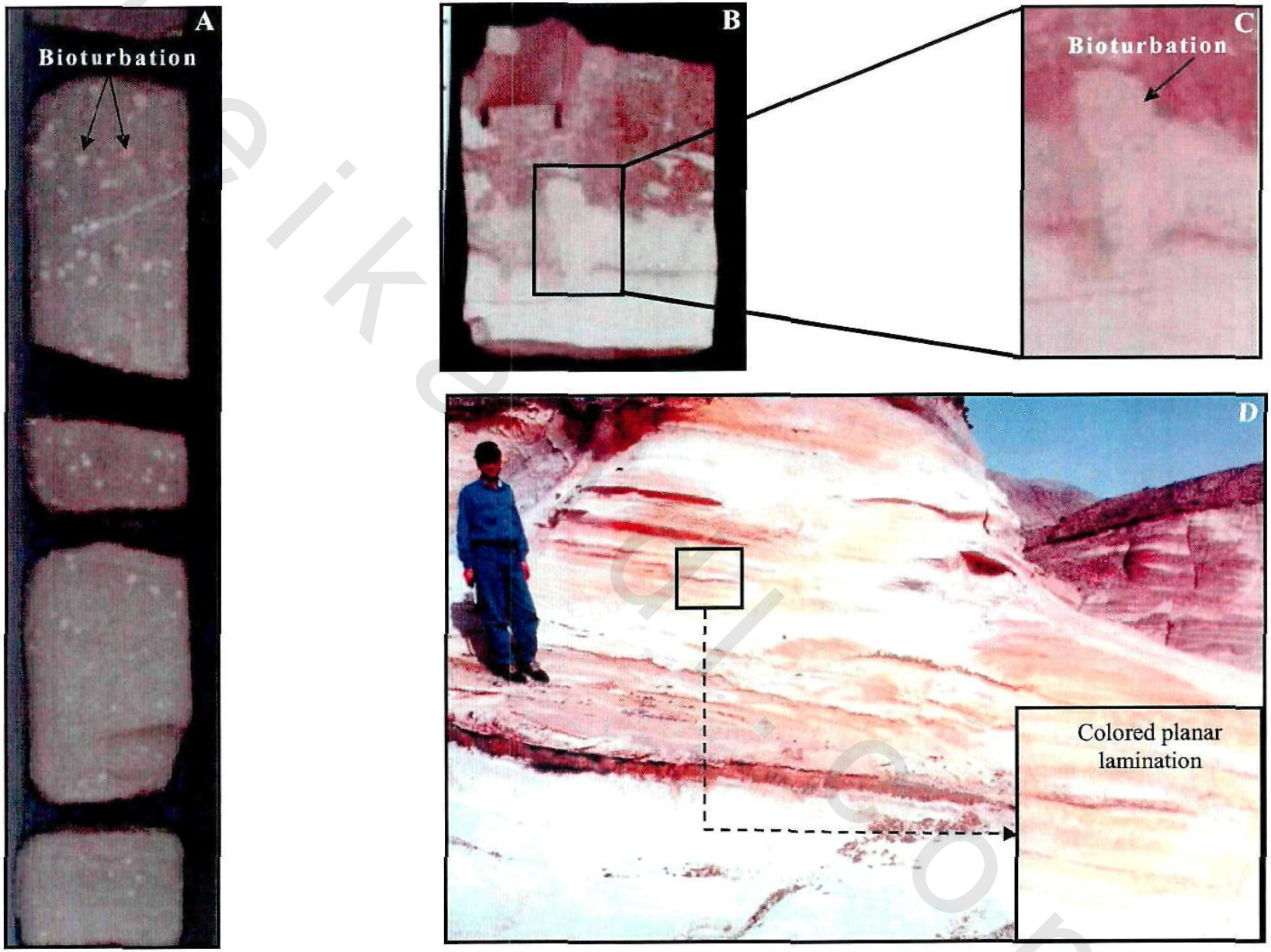
A
Bioturbation
B
C
Bioturbation
D
Colored planar lamination

Plate 3.6

A, B) Channel structure filled by fine grained, tangential tabular cross bedded sandstone. Base of Naqus Formation.

C) Massive sandstone bed displaying no obvious sedimentary structures. Note calcite filled fractures. Naqus Formation.

D) Content and coarse tail normal grading marked by an upward decrease in grain size. Naqus Formation.

Plate 3.6

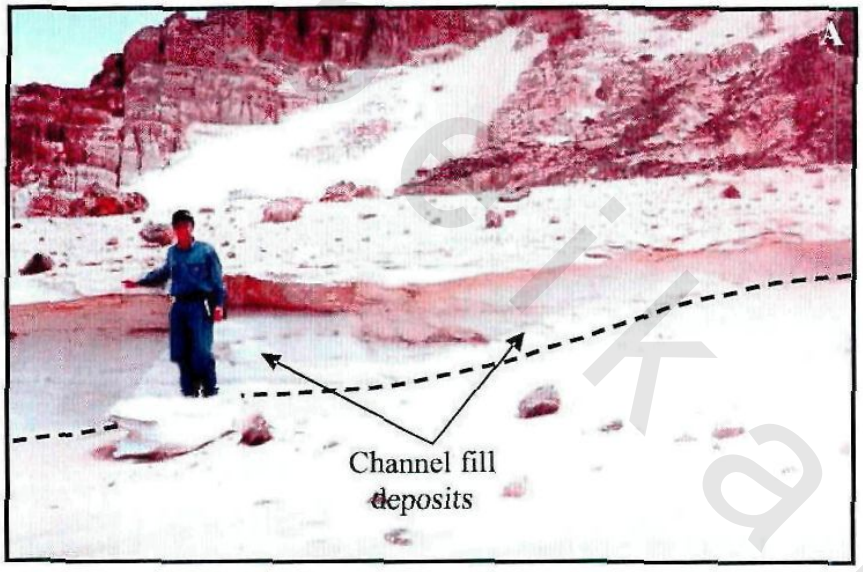
A
Channel fill
deposits

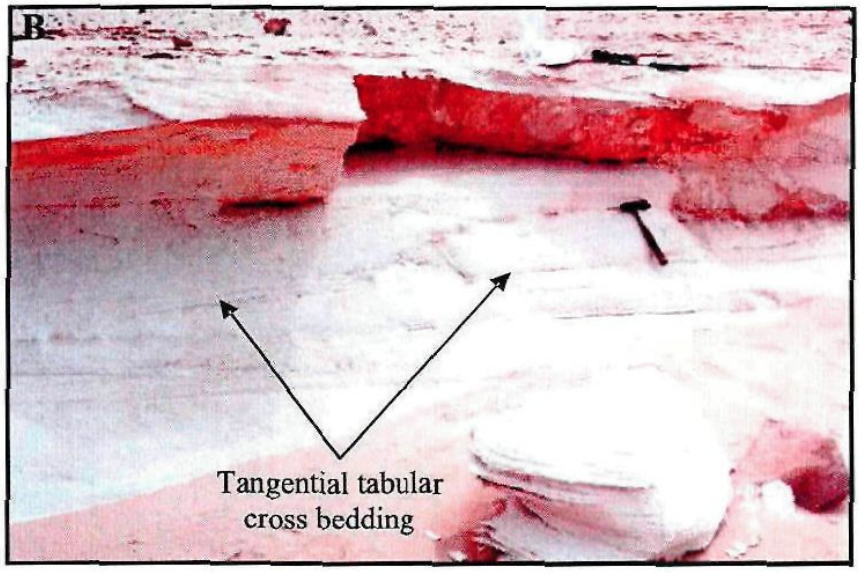
B
Tangential tabular
cross bedding

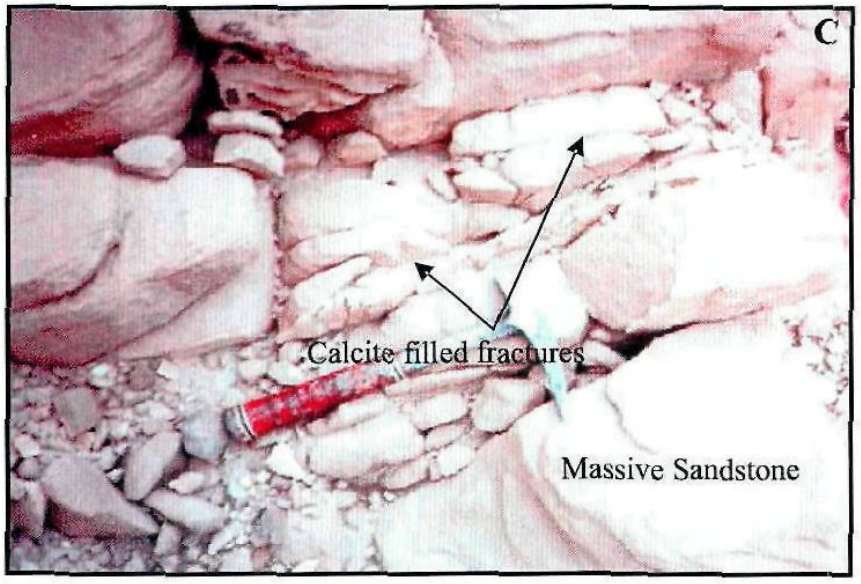
C
Calcite filled fractures
Massive Sandstone

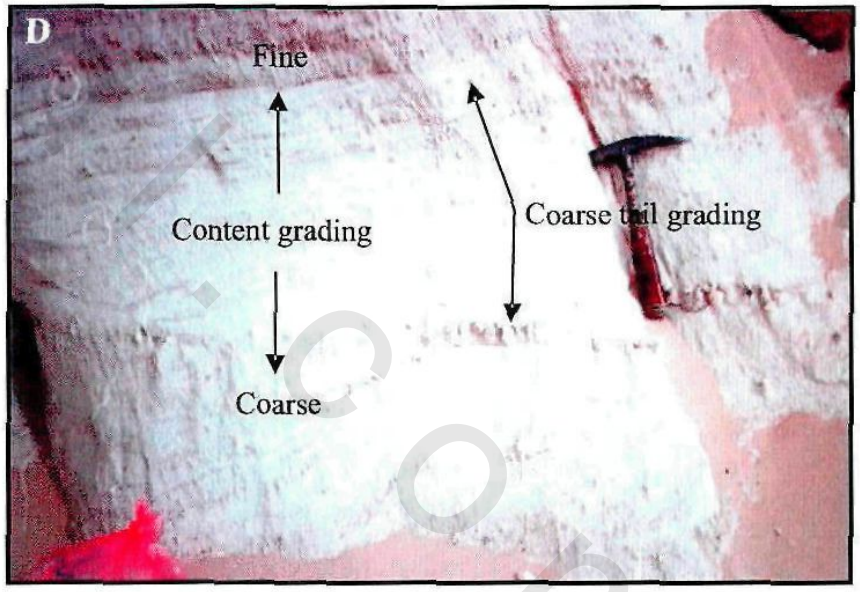
D
Fine
Content grading
Coarse
Coarse tail grading

Plate 3.7

A) Content and coarse tail normal grading in a planar tabular cross bedded sandstone. Elongated to rounded pebbles and cobbles are mixed with sand grains of other size grades. Naqus Formation.

B) Planar lamination and differential weathering. Naqus Formation.

C) Planar lamination and vertical jointing. Naqus Formation.

D) Planar laminated sandstone overlain by massive sandstone. RB-A5 well, depth 12247.60-12248.25 ft.

E) Planar lamination. RB-A5 well, depth 12262.85-12263.30 ft.

F) Planar tabular cross bedding. RB-C2 well, depth 12259.00-12260.20 ft.

G, H) Planar tabular cross bedding paved by mud drapes. RB-C2 well, depths 12306.40-12306.75, 12307.55-12307.85 ft, respectively.

Plate 3.7

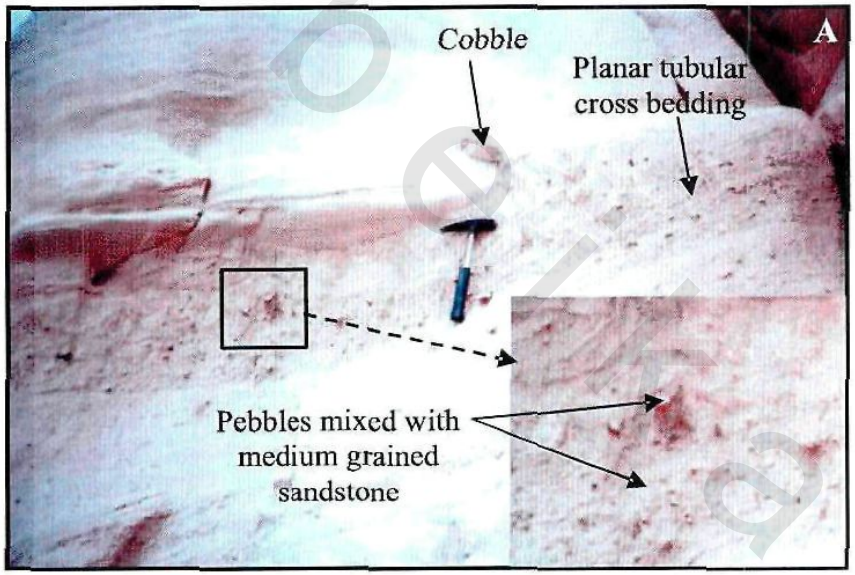
A
Cobble
Planar tubular cross bedding
Pebbles mixed with medium grained sandstone

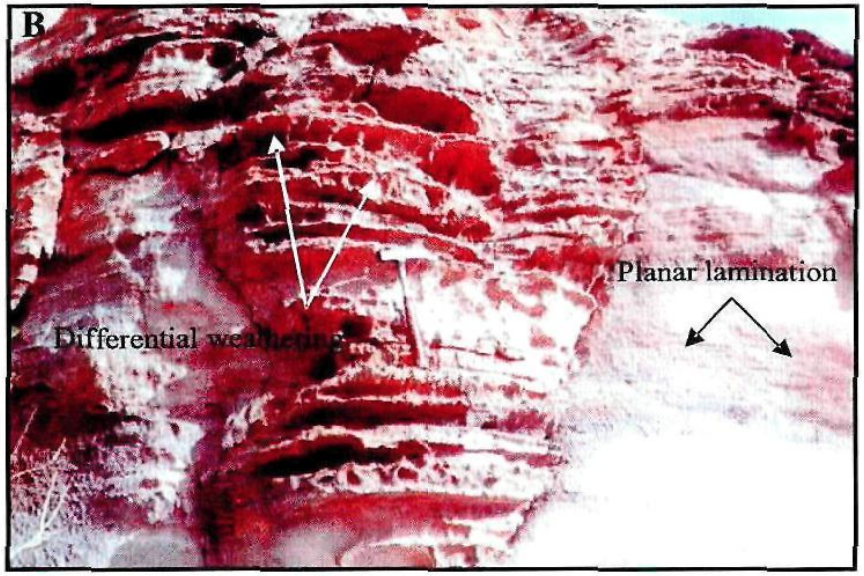
B
Planar lamination
Differential weathering

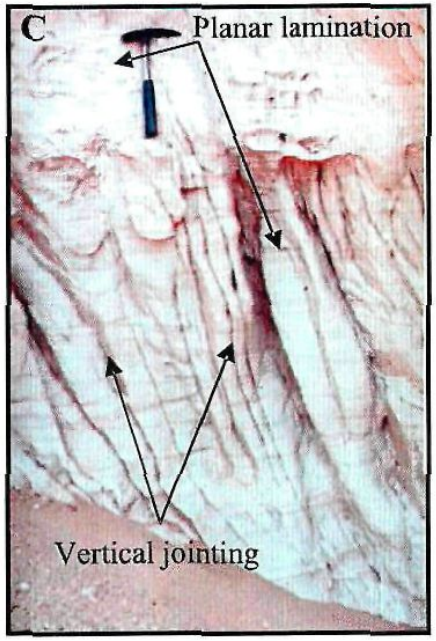
C
Planar lamination
Vertical jointing

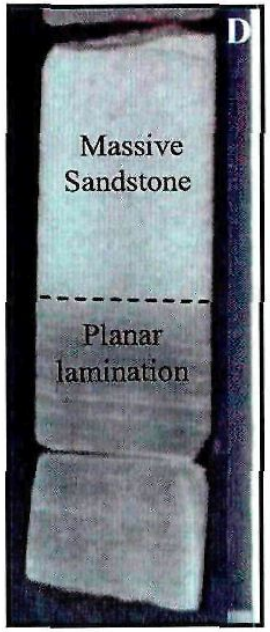
D
Massive Sandstone
Planar lamination

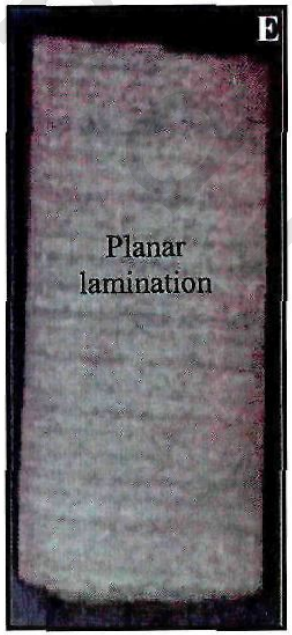
E
Planar lamination

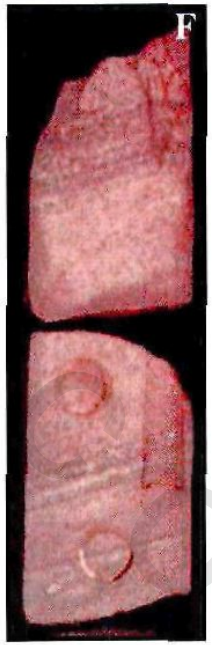
F

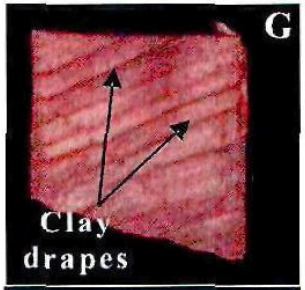
G
Clay drapes

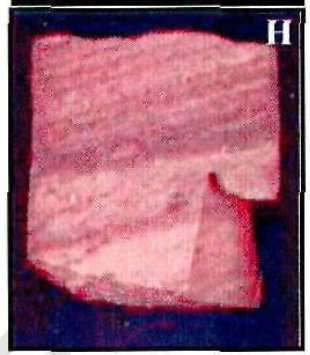
H

Plate 3.8

A) Planar tabular cross bedding and differential weathering. Naqus Formation.

B) Planar tabular cross bedding and vertical jointing. Naqus Fm

C) Tangential tabular cross bedding. Araba Fm

D) Faulted bedding and undulated lamination. Naqus Formation.

Plate 3.8

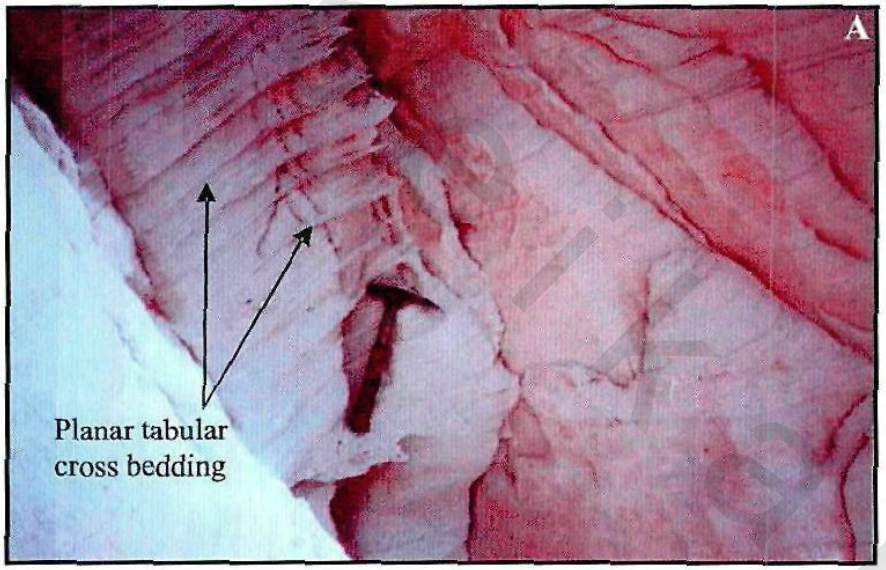
A
Planar tabular
cross bedding

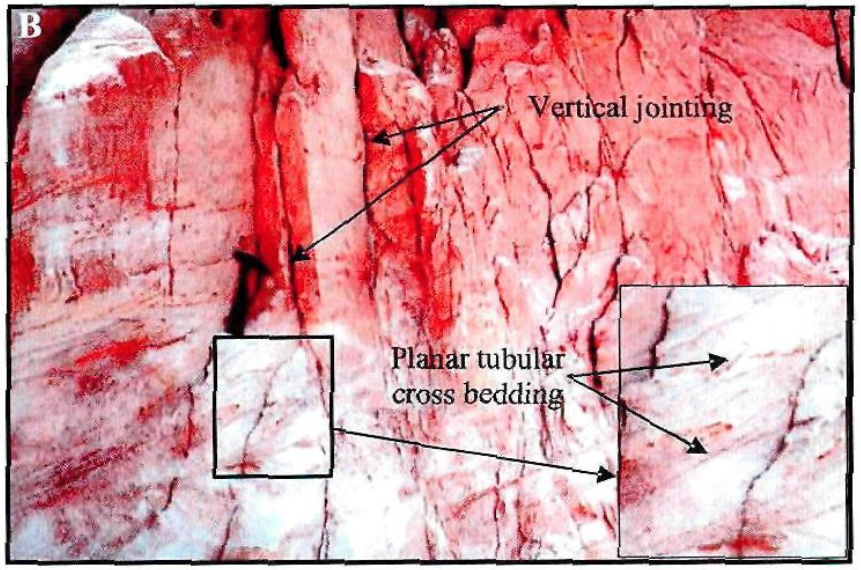
B
Vertical jointing
Planar tubular
cross bedding

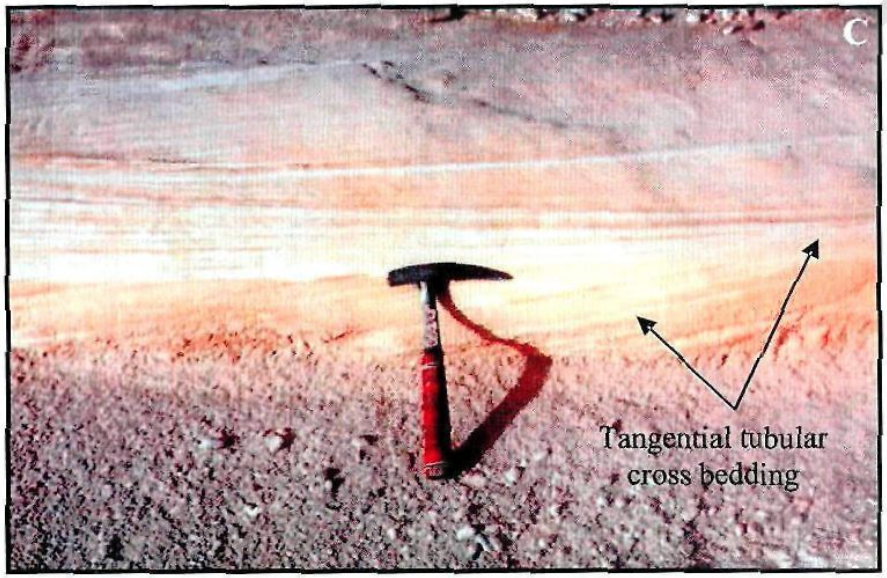
C
Tangential tubular
cross bedding

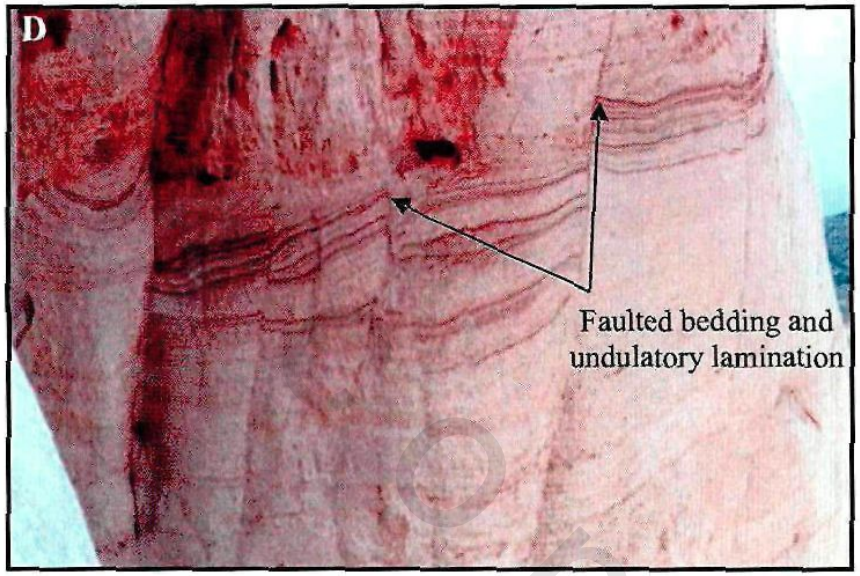
D
Faulted bedding and
undulatory lamination

Plate 3.9

A) Flaser lamination. RB-C2 well, depth 12351.00-12352.00 ft.

B) lenticular lamination. RB-C2 well, depth 12314.50-12316.00 ft

C) Wavy lamination. RB-C2 well, depth 12298.00-12298.80 ft.

D) Cross lamination. RB-C2 well, depth 12285.00-12285.90 ft.

Plate 3.9

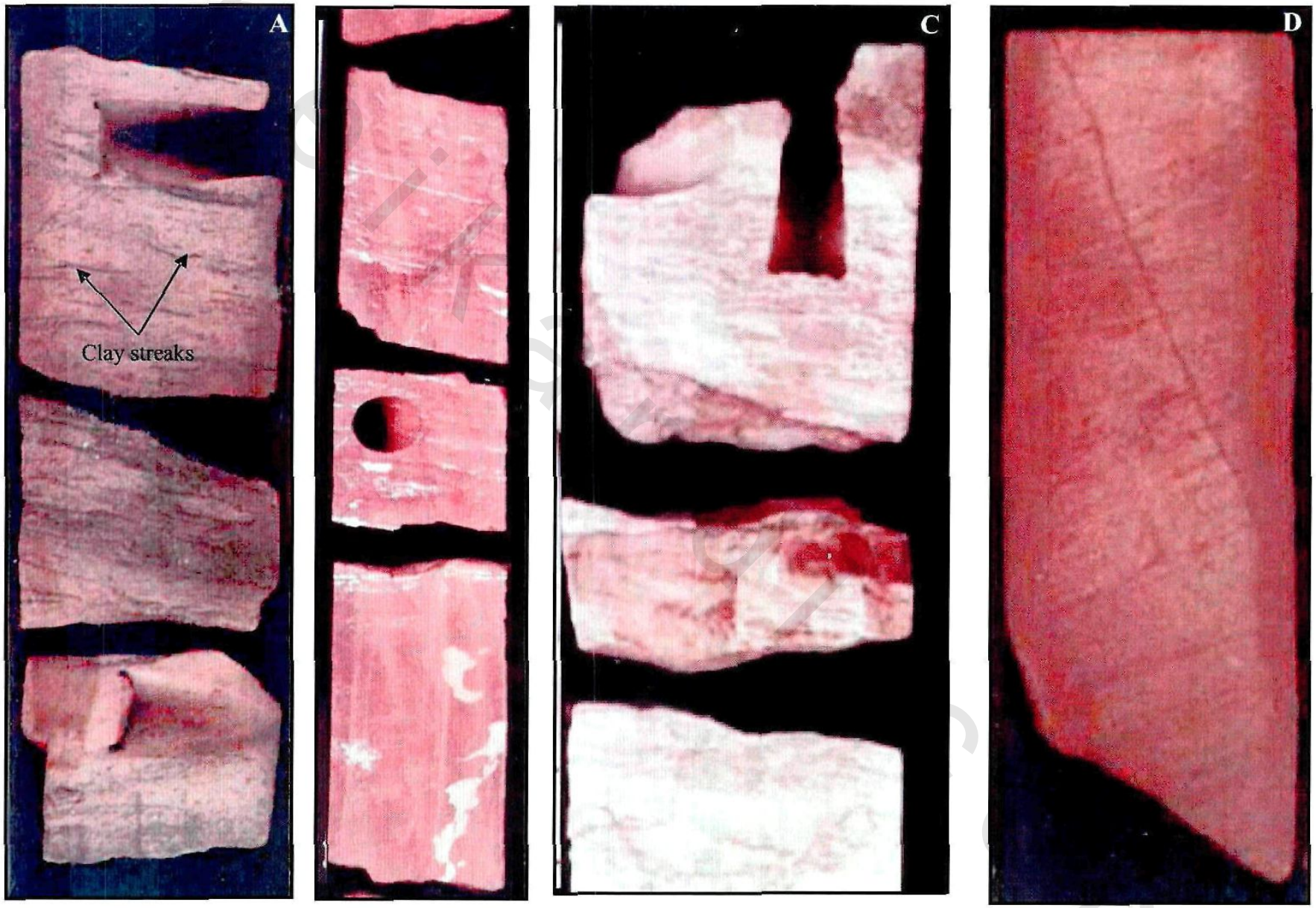

Plate 3.10

A) Convolution and undulatory lamination. Naqus Formation.

B) Convolution. Naqus Formation.

C) Convolution and recumbent foresets. Naqus Formation.

D) Differential weathering due to wind action. Naqus Formation.

Plate 3.10

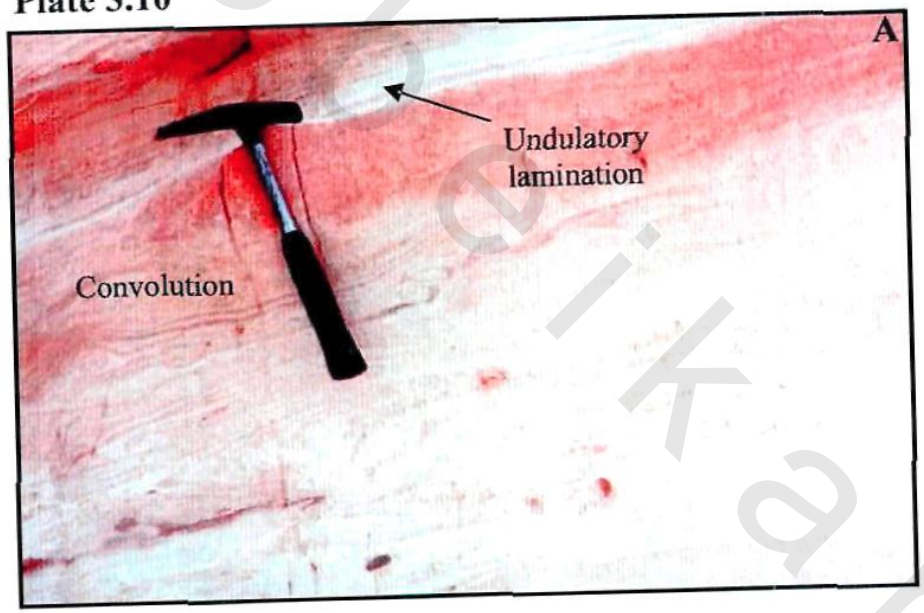
A
Undulatory lamination
Convolution

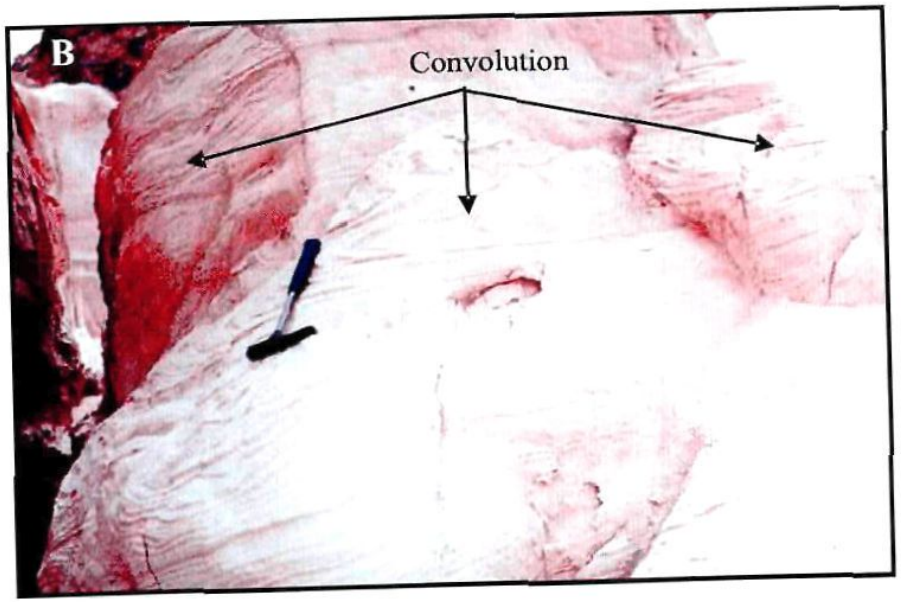
B
Convolution

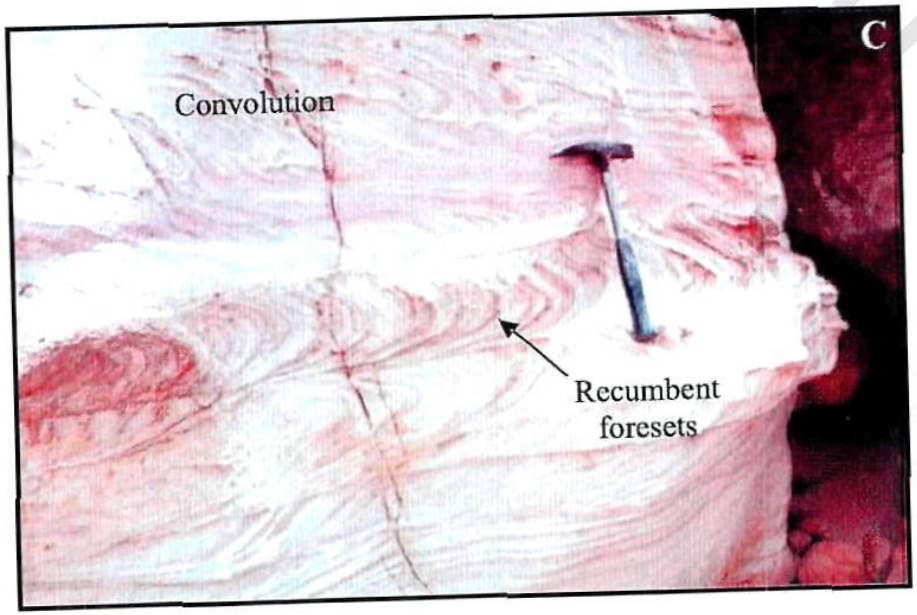
C
Convolution
Recumbent foresets

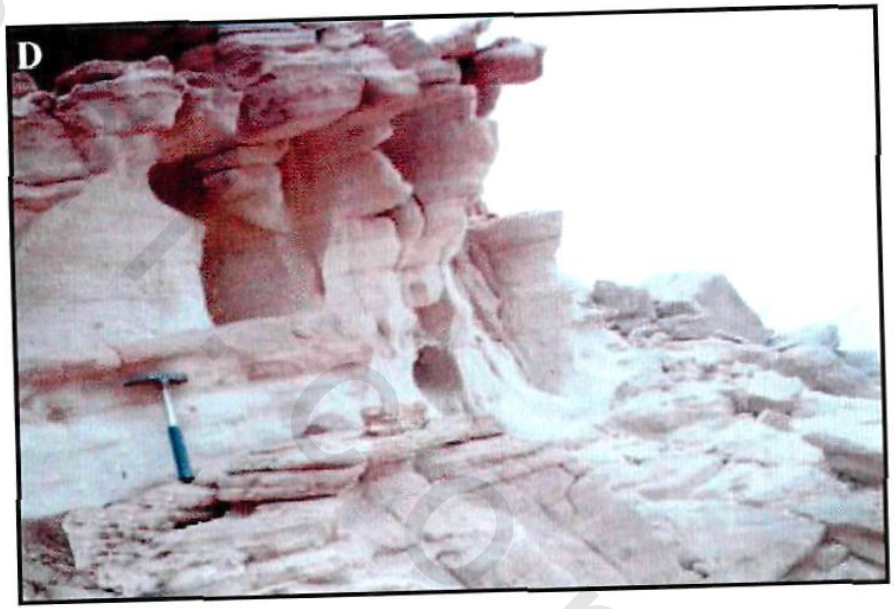
D